Insect eye solar tracking

Nayer Naiem Aziz Abdalla Youssef

Thesis to obtain the Master of Science Degree in

Energy Engineering and Management

Supervisors: Prof. Luís Filipe Moreira Mendes

Prof. Thomas Haalboom

Examination Committee

Chairperson: Prof. José Alberto Calado Falcão de Campos

Supervisor: Prof. Luís Filipe Moreira Mendes

Member of the Committee: Prof. Horácio João Matos Fernandes

September 2015

Acknowledgements

I will begin by giving my special thanks to Prof. Thomas Haalboom for his great efforts and valuable time with me in the project. Also, I would like to thank Prof. Filipe Mendes for guiding me in the project all the way from Lisbon, Portugal. Furthermore, thanks to Eng. Mohamed Abuelnour, Eng. Ahmed Schekeb Raoufi for their help in the project. Thank you for supporting me with your great potentials and teaching me new techniques in many fields by your great experience.

Also I want to thank my family for their patience, support and giving me the splendid opportunity to do my Masters abroad.

Abstract

It is well known that solar tracking systems increase solar panel efficiency. The higher demand for energy production requires more efficient systems to harness more energy for useful use. Cloudy weather conditions reduce the solar panel's energy production significantly. The center of study in this thesis is the development and experimentation of an artificial compound insect eye for maximum solar radiation detection even in cloudy conditions to know the best orientation of the solar panel for maximum capture efficiency.

Photodiodes were used as the eye's sensing unit. Printed circuit board were used to connect these single photodiodes. Arduino Mega 2560 was used as the brain to collect data and send them to a computer for monitoring. A hemi-spherical eye was designed using Solidworks and manufactured using a 3D printer Ultimaker 2. The Arduino program mapped the photodiodes to the final output image correctly and used a multiplexer circuit to rotate on all photodiodes. Connection problems aroused and a pervious prototype sensor was used to prove the concept. The sensor was successful in determining the maximum point of radiation even in cloudy conditions where the solar panel's power output increased by 6% by orienting it to the point of maximum radiation given by the eye instead of fixing it in a horizontal position, which is a significant number when applied to large solar power stations.

Key Words: Solidworks, Photodiode, Artificial Insect Eye, Flexible Circuit, Solar Panel, Solar Tracking.

Resumo

O aumento da procura de energia suscita a necessidade de sistemas mais eficientes para a sua transformação. É bem conhecido que os sistemas de seguimento solar aumentam a energia captada pelos painéis solares assim como que as condições de céu enevoado reduzem significativamente a sua produção. O objetivo deste trabalho é desenvolver e testar um olho composto artificial para a detecção da direção da radiância solar máxima, mesmo em condições de grande nebulosidade, e desta forma orientar corretamente os coletores solares e maximizar a captação de energia.

Os sensores unitários utilizados na criação do olho composto são fotodíodos que foram ligados a uma placa de circuito impresso. O Arduino Mega 2560 foi usado como cérebro, para recolher os dados e os enviar para um computador para monitorização. O olho hemisférico foi criado através do uso do Solidworks e de uma impressora 3D. Foi utilizado um multiplexador para recolher sequencialmente o sinal dos fotodíodos e o programa usado no Arduino produziu o seu respetivo mapeamento. O protótipo desenvolvido apresentou alguns problemas de construção e um sensor já existente foi utilizado para testar o conceito pretendido. Este sensor conseguiu determinar o ponto de máxima radiância com sucesso em condições de grande nebulosidade e o painel solar usado no teste teve um aumento de 6% na sua produção elétrica ao ser orientado da posição horizontal para a direção indicada pelo sensor, o que indica um potencial de aumento de produção, principalmente em grandes centrais.

Palavras-chave: Solidworks, Fotodíodo, Olho de Inseto Artificial, Circuitos Flexíveis, Painel Solar, Seguimento Solar

Table of Contents

List of Figures

List of Tables

List of abbreviations

CAD	Computer Aided Design
FDM	Frequency Division Multiplexing
GPS	Global Positioning System
LED	Light Emitting Diode
PCB	Printed Circuit Board
SLS	Selective Laser Sintering
SMC	Surface Mount Components
SMT	Surface Mount Technology
TDM	Time Division Multiplexing
THT	Through Hole Technology
TSI	Extraterrestrial Irradiance
TTL	Transistor-Transistor Logic
VLSI	Very Large Scale Integration

Chapter 1

Introduction and Problem formulation

1.1 Introduction

Nowadays there has been a higher demand of energy production and the depletion of fossil fuel reserves has caused the search for an alternate source of power that is renewable and sustainable. Solar power is one of the best alternative power sources as it is abundant in nature and a renewable form of energy. For harnessing solar radiation, photovoltaic panels have been developed and used throughout the years.

Nature has been one of the most inspiring environment for the majority of engineers, scientists, and designers. From the beginning of human history, it has played a vital role in our creative expression. The lands and waters we rely on for daily survival shape how we view and interpret the world around us. And in turn, the art we create from nature's inspiration becomes part of our personal and cultural identity. Insects, animals, and plants are nature's version of mechanical, mechatronic and energy systems, so studying how these creatures evolved through ages, investigating their different mechanical, energy, chemical, and even neurological systems, and observing their response to different stimuli can be a great inspiration for developing solutions to many problems faced in life. [1]

Since many of the mechatronic energy systems developed nowadays are already inspired by nature and its creatures, such as plane and automotive aerodynamics and many mechanical motion systems, further bio-inspired research and observation will definitely broaden horizons to new approaches for implementing more advanced and complex mechatronic systems. This is the study of bionics. Often, the study of bionics emphasizes implementing a certain function found in nature rather than just imitating the exact biological structure.

In the area of solar tracking, cloudy weather conditions reduce solar panel’s energy production significantly [8]. So to try and gain the maximum output of a solar panel in this fact into consideration, an insect eye sensor was developed to detect the maximum point of irradiance in cloudy conditions and orient a solar panel to that point.

The thesis is organised as follows: the first chapter is introducing the thesis idea, the research that tackled this idea and the project aim. Chapter 2 shows the background knowledge that is needed to be able to work in this project. Chapter 3 shows the manufacturing of the sensor and building up the solar tracker. Chapter 4 shows the results and problems faced in the project. And finally chapter 5 shows the conclusion and also the future recommendations for this project.

1.2 Project Aim

Engineering an artificial compound eye is a challenging task, since the angle and alignment of each photoreceptor unit is very important and affects greatly the final output. The center of study in this thesis is the development and experimentation of an artificial compound insect eye for maximum solar radiation detection even in cloudy conditions to know the best orientation of the solar panel for maximum capture efficiency. The reason behind the name compound eye is because they are made up of repeated units, the ommatidia, each of which functions as a separate visual receptor. A single compound eye may consist of thousands of ommatidia located on a convex surface, forming the eye structure, and thus each pointing in a slightly different angle and direction. Although every ommatidium has its own optical and receptor structure, the image perceived is a combination of inputs from every ommatidium in the eye, and thus giving the eye its properties.

However, compound eyes have limited resolution compared to humans' eyes. Since each individual lens is of very small size, diffraction imposes a great limitation on the eyes resolution, and as a result, a compound eye with comparable resolution to our simple eyes needs to be of approximately 11 meters diameter. Insects' compound eye is the structure to be discussed in this thesis. [1]

A spherically shaped structure with photo-detector sensors implemented on its surface will represent the sensing element. Moreover, a 2 degree of freedom rotary motion system will be implemented to direct the panel to the correct angle.

1.3 State of the art

There has been a lot of research going on in the area of solar tracking and tracking of the sun even on cloudy days.

The first part is about the study of the number of axis for solar tracking. There are two ways, single axis and dual axis solar tracking. Single axis is simply moving the panel in only one degree of freedom and dual axis is moving the panel in 2 degrees of freedom. In general solar tracking gives higher efficiencies compared to fixed tilt panels. Dual axis tracking is more efficient than single axis tracking. [2]

Since the aim of solar tracking is to generate more power. It is important to take into consideration that the power consumption of the tracking system should be low. [3]

The second part is the control strategy. There 2 major types of solar tracking strategies, the open loop control strategy and the closed loop control strategy. An open-loop controller uses only the current state and the algorithm of the system to compute its input into a system without using feedback to determine if its input has achieved the desired goal. It is simpler and cheaper than the closed-loop type of sun tracking systems. There is no observation of the output of the processes that it is controlling like in the closed loop controller. Therefore, an open-loop system doesn't have the

ability to correct any errors so that it can compensate for disturbances in the system. Closed-loop controllers of solar tracking systems are based on feedback control. Sensors give a number of inputs which detect relevant parameters by the sun to a controller, then manipulated in the controller and yield outputs. [4]

There is also the hybrid control strategy, which is made by the combination of open loop tracking strategies based on solar movement models and closed loop strategies using a dynamic feedback controller, a hybrid tracking system is made. The advantage of the hybrid tracking is that it is cheaper than closed loop tracking with almost the same efficiency. A comparison with open loop control is shown figure 1-1. [5]

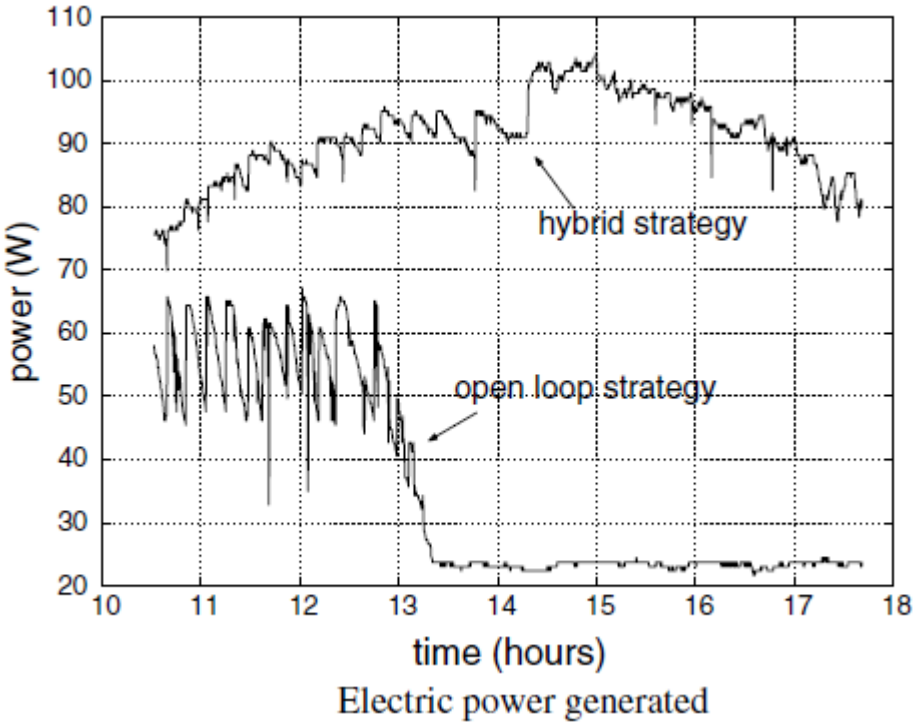

Figure 1-1 Experimental results using an open-loop and the proposed hybrid strategy. [5]

The third part was to know where the maximum radiation is coming from to be able to point the solar panel perpendicular to that radiation for maximum power output. Most sensors developed today work well in tracking the sun on clear skies, one way is using the combination of astronomical estimates from GPS and vision-sensor image processing. By using image processing, a decision making process is used to differentiate if the current weather condition is sunny or not [6]. The solar tracking system decides whether to use the image processing outcomes or astronomical estimates based on the output. For the tracking method that combines the solar image and astronomical estimates, the solar panel can maintain a normal direction to sunlight. But, in cloudy weather conditions, solar image controlling is not the best case due to the difficulty in locating the sun using images; In that case, operating only using astronomical estimates only is used for tracking. [6]

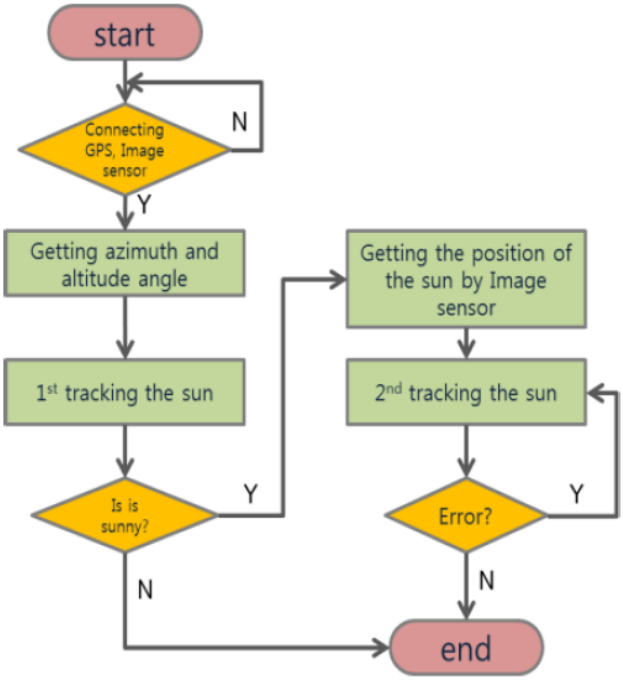

Figure 1-2 Tracking flow chart [6]

Other ways is to track the beam radiation other than image processing is using sensors such as Pyranometers [7]. In cloudy conditions, the diffuse component in the global radiation contributes by a significant amount and acording to [8] the energy capture decreases by 23% of the maximum efficiency that can be reached by the solar panel because of inadequacy in capturing most of the diffuse radiation. A controlled tracking system that tracks beam radiation in clear skies and fixes the panel in horizontal position during cloudy conditions has shown to increase the capture efficiency. This is a different method to deal with cloudy conditions than using the astronomical estimates to track the sun on cloudy days.

So in this thesis, a sensor was developed for maximum solar radiation detection in cloudy conditions to know where the maximum radiation is coming from and orient the panel accordingly. The manufactured sensor was hemispherical in shape and had 92 photodiodes. Unfortunately, that prototype experienced some connection problems due to manufacturing, so it gave inconsistent results. As a result, a previous prototype at the DHBW Karlsruhe was used as a proof of concept.

The previous prototype insect eye was made for the purpose of following light indoors and its design was relatively different than hemispherical one. The angle and alignment of each photo receptor unit is very important and affects greatly the final output. The photodiode light sensor was chosen as the detector was successful to represent insect’s eye ommatidium to simulate different proprieties of the eye. A micro-controller represented the insects' brain that collects the signals sent from the photodiodes and combine them together to give an output image of the surrounding (32

pixels). Moreover, using 3D printing technology to build the eye model was efficient enough in dimensions aspect. [9]

This prototype was used as a proof of concept to see the reaction of the eye in sunny and cloudy conditions, but it was not integrated with the solar panel movement as its design would not give consistent results. The panel power output was compared in the horizontal position and the oriented position given by the eye. Figure 1-3 shows the shape of the previous prototype eye. [9]

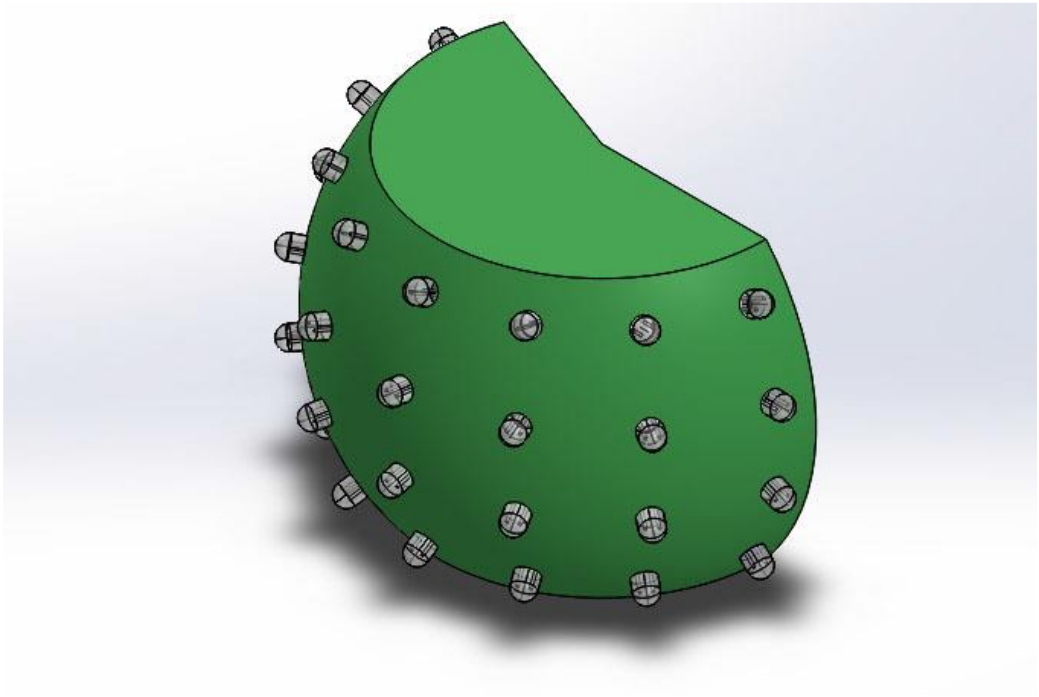

Figure 1-3 Previous prototype eye [9]

Chapter 2

Background

The purpose of this chapter is to show the background knowledge that is needed to be able to work on this project. Many things have to be put together to work on the project: 1) Eye types, 2) Light sensor types, 3) Microcontrollers, 4) Multiplexing, 5) Flexible circuits, 6) 3D-printing, 7) Solar Irradiance and 8) Solar Cells.

2.1 Eye types

Eye types can be divided into two types, human eyes, which have one concave surface containing all photo receptive cells, and compound eyes, which are composed of many photo receptive units called ommatidia, laid out on a convex surface. The compound eye is what will be used in this thesis. It was briefly compared to the human eye in the end of this section. Moreover, a comparison was made between different types of compound eyes. [10]

2.1.1 The compound eye

In arthropods, in annelids and some bivalve mollusks commonly have compound eyes. Thousands of individual photo reception units consist the compound eye. The combination of inputs from the numerous ommatidia (individual "eye units") gives an image, located on a convex surface, consequently pointing to some extent in different directions. The way pigment is distributed between ommatidia in the structure of a compound eye, the eye can form either superposition images or apposition images. [11]

2.1.1.1 Ommatidia structure

An Ommatidium contains a cluster of photo receptive retinual cells surrounded by support and pigment cells. The outer part of the ommatidium is cover by a transparent cornea. The brain receives one independent picture element from every ommatidium, from which it forms one image. The number of ommatidia vary according to the type of insect. It varies from a handful in some primitive insects to about 30 thousands in dragon flies.

Ommatidia are typically hexagonal in cross section and approximately ten times longer than wide (Figure 2-3). The diameter is largest at the surface, narrowing towards the inner end. At the outer surface there is a cornea, below which is a pseudo cone that acts to further focus the light. The cornea and pseudo cone form the outer ten percent of the length of the ommatidium. The inner 90% of the ommatidium contains 6 to 9 (according to the species) thin and long photo receptor cells tightly packing the ommatidium. [12]

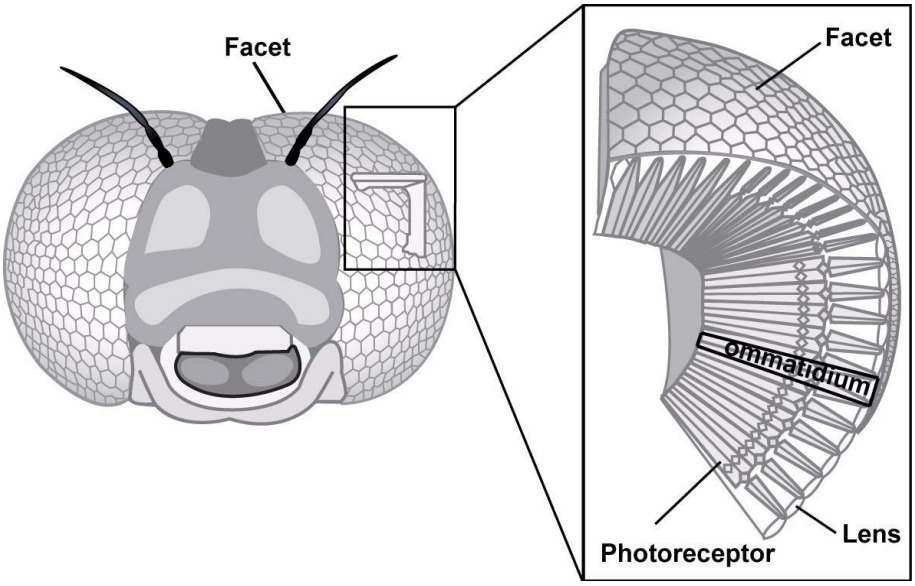

Figure 2-1 Compound Eye Structure [10]

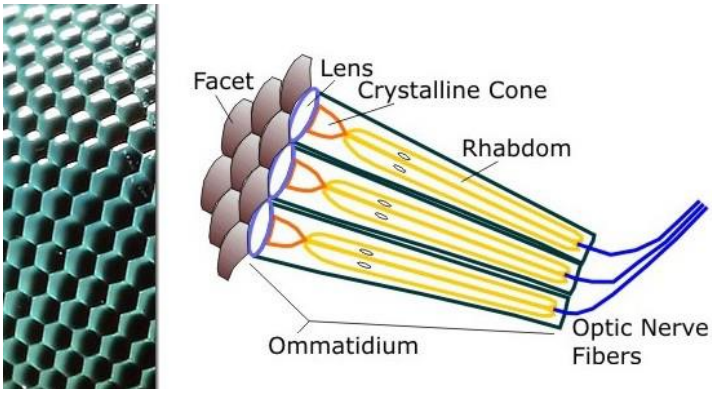

Figure 2-2 Ommatidium Structure [10]

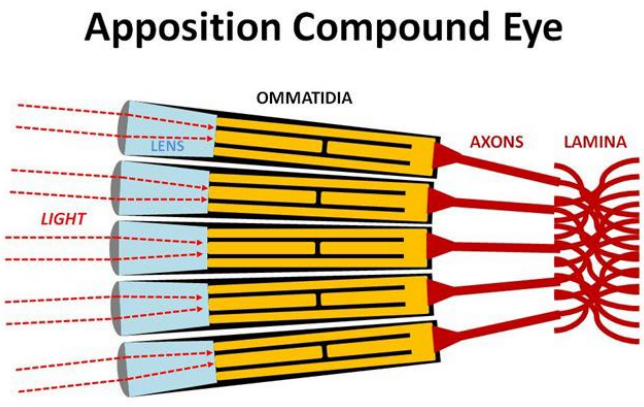

Figure 2-3 Apposition Compound Eye [13]

2.1.1.2 Apposition Eye

In the apposition eye, each ommatidium focuses only rays that are nearly parallel to its long axis, so that each forms an image of only a smaller part of the visual field. The whole image results from a combination of these smaller images. Apposition eye insects, such as drone (male) bees and dragon flies, have areas with acute vision characterized by larger facets which help alleviate the effects of diffraction. Foveal vision in birds is similar to this acute vision portion of the eye. [10]

2.1.1.3 Superposition eye

In a superposition eye, the ommatidium sensory cells can sense light from a large part of the visual field so that as many as 30 neighboring ommatidia images may overlap with that image received. The superposition image loses in sharpness but gains in brightness when compared with the apposition image. However, by movement of pigment between the ommatidia, some insects have the capability to temporarily change between one eye type to the other to allow adaptation in the dark. Light is refracted through the lens in the refraction superposition eye element of each ommatidium in such a way that it arises at the same angle from the bottom of that ommatidium, and then onto a small retina. The ommatidium realizes this by acting like a two-lens telescope, which it does by containing a cylindrical lens with a graduated refractive index that continually bends the light as it travels through the tube. In other words, the refractive index of the lens varies depending on where it is along the tube. [10]

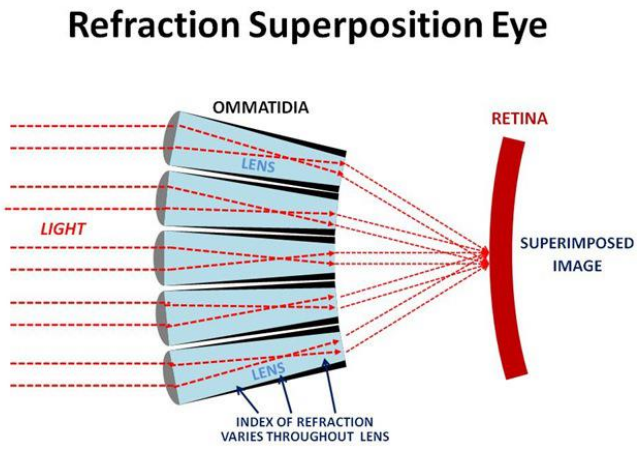

Figure 2-4 Refraction Superpositon Eye [10]

In the reflection superposition eye, the insides of ommatidia are mirrored, and each facet uses reflection internally to focus the image onto the small retina. This eye type is common among marine creatures, such as lobsters that live in light-poor environments in which image formation is improved by superposition but refractive lenses are trickier to effect in water, which has a higher refractive index than air. Via reflection, the eye achieves superposition. [10]

Similar to the apposition eye is the neural superposition eye in a way that after the images were received by the 8 rhabdomeres, or photo receptor cells, they were combined into a single rhabdom which was connected by a single axon, or nerve fiber, to the lamina, or top nerve layer below. However, the rhabdomeres stay separated clear down the tube in the neural superposition eye, and emerge from the bottom as 7 separate fibers, each of which is then joined at the lamina to 6 other fibers from rhabdomeres from the 6 adjoining facets neighboring it which are angled in the same direction so the image received at the lamina is 7 times more bright than the image at any given photo receptor, which aids flies form superior images in low light conditions. And the shape of the eye doesn't need to be as strictly spherical because superposition is achieved via wiring (vs. optics), allowing for greater flexibility of form. Neural superposition eyes are also believed to be more sensitive to motion detection than apposition eyes and might experience an improved signal-to-noise ratio.

2.1.2 Comparison

Compared with human eyes [14], compound eyes possess a very large view angle, and can detect fast movement and, in some cases, the polarization of light. On the other hand, compound eyes have poor resolution so they are not good at making out detail. Insects that can fly well, such as honey bees and flies, or that catch prey, such as dragonflies or preying mantis, have specialized zones of ommatidia. These zones are organized into a fovea area that gives acute vision. In the acute zone, the eye is flattened and the facets are larger, which allows more ommatidia to receive light from a spot and thereby achieve higher resolution.

Compound eyes generally allow only a short range of vision. For example, flies and mosquitoes can see only a few millimeters in front of them with any degree of resolution, although within this short range they can see detail that we could see only with a microscope.

Dragonflies have one of the most elaborate eyes of any insect, capable of pinpointing the motion of a small prey insect several meters away, even while the dragonfly is traveling fast. Butteries have color vision that is more enhanced than our own, enabling them to locate food from flowers. Honey bees can see in ultraviolet, which allows them to perceive patterns on nectar-laden flowers that are invisible to us. Many insects, including bees, can also detect polarized light, which they use in navigation. A compound eye is what was used in this thesis.

2.2 Light sensor types

Light sensors convert light energy to an electrical signal output. When converted into electrical energy, the beaming energy within the infrared to ultraviolet light frequency spectrum source can be measured. [15] An important part of this project's realization was choosing the detector to use for this solar tracking application. The choices seemed overwhelming; photodiodes, phototransistors, photodarlingtons, photomultiplier tubes, photoresistors, various hybrids, LED’s as detectors and even thermopiles. Light sensing applications differ widely from specialized scientific instrumentation that

needs to detect separate photons to systems that control high speed welding and cutting lasers that produce kilowatts of optical power.

Fortunately, there are sensors for nearly any application: from a photomultiplier tube which gives a large voltage for every photon it detects, to cooled thermopiles that absorb kilowatts of power providing a thermocouple voltage that is proportional to the optical power absorbed. To reach an efficient choice of what detector to implement in the actual build, a detailed comparison was carried out between different light detectors. Finally, the chosen sensor was the one matching most of the required properties suitable for the implementation.

Table 2-1 Comparison table between some light sensors [15] [16] [17] [18]

Electrical Characteristics	Photodiodes	Phototransistors	Photoconductors	Photomultiplier tubes
Available Wavelength(μm)	0.2-2.0	0.4-1.1	2-15	0.2-0.9
Sensitivity	Very Good	Very Good	Very Good	Excellent
Linearity	Excellent	Good	Good	Good
Ambient Noise Performance	Very Good	Very Good	Very Good	Fair
Dynamic Range	Excellent	Very Good	Good	Very Good
Stability	Very Good	Good	Fair	Very Good
Reproducibility	Excellent	Fair	Fair	Fair
Cost	Low	Very Low	High	High
Ruggedness	Excellent	Excellent	Good	Poor
Physical Size	Small	Small	Small	Large

2.2.1 Photodiodes

Figure 2-5 Photodiode [19]

They are light sensitive semiconductor devices, manufactured essentially the same way as simple semiconductor diodes. The main difference is that photodiodes are larger and are packaged in a way allowing light to enter the sensitive area of the diode. They have many advantages making them practical for many applications. [20]

- They can easily measure from pico-watts to mill-watts of optical power
- Depending on the semiconductor material used, they can detect wavelengths from 190 to > 2,000 nm
- They are small and light weight
- Almost any photo-sensitive shape can be fabricated
- They have very reproducible sensitivity
- They can be very responsive, with rise-times as fast as 10 picoseconds

A pre-amplifier is required for Photodiodes to give signal gain for applications to detect pico-watts of light power. But for high optical power levels of less than 10 microwatts, good performance can be given by a simple load resistor configuration and "TTL" compatible voltage swings. Silicon based Photodiodes cover the wide range of wavelengths from 190 to 1100 nm (the lower limit is set by absorption of ultraviolet light in air). Germanium (Ge) Photodiodes overlap the silicon response spectrum and are usable to about 1600 nm. Compounds of antimonide, arsenide, gallium, indium, and phosphorous that form semiconductors can be specially fabricated to cover small sections of the 190 to 2000 nm spectral range. For example, the fiber optics industry uses indium-gallium-arsenide (InGaAs) detectors for the 800 to 1800 nm range. More expensive photodiodes can sense energy much further out in the IR spectrum. This THT photodiode was the one chosen to be used in the previous prototype, it has a responsivity angle of 70 degrees.

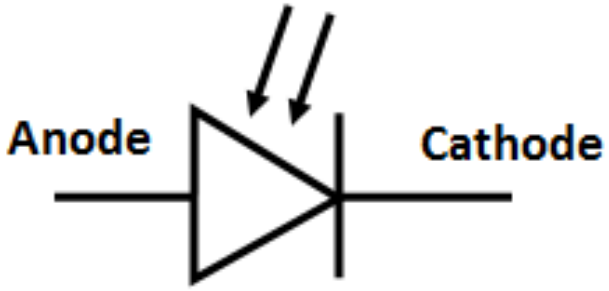

Figure 2-6 Photodiode schematic

2.2.1.1 Through Hole Technology (THT)

THT is the mounting method which is used in electronic components since 1980s. It uses leads on the components that are inserted to holes drilled in printed circuit boards (PCB) and soldered to pads on the other side. Through Hole Technology has some advantages over Surface Mount Technology such as reliability. TH-Technology are more advantageous in high reliability circuits which needs stronger connections to layers. Surface Mount Technology secures its components by mere solder on the surface of the printed circuit board. As the pin of the electronic component goes through the board it allows the components to bear more environmental stress. This is perfect in circuits or products where very high temperatures, accelerations or collisions occur. THT can be easily used in normal breadboards. Therefore, they are also useful in prototyping as it is easy to manually adjust them. In addition many Through Hole components are less expensive compared to surface mount components [21].

There are two types of TH-components: radial and axial lead components. The radial lead components stand out of the board, as its pins are on one side of the component. It is used when snugness to the board is needed. After mounting radial components they tend to stand up in a perpendicular way to the PCB. They are hence fit in high density PCBs as they occupy less surface area. They are also easily mounted on PCBs which makes them perfect for Auto mounting. On the other hand the axial leads they run through a component axially. Each pin of the wire exits the component from an end. This type needs two separate holes in the PCB to allow the component to fit. They usually are a cylindrical or box shaped components [21].

Through Hole Technology in general requires drilling holes in the PCB which is both expensive and time consuming. The main disadvantage of these holes is that it reduces the routing area in all layers from top to bottom layers which is a great disadvantage in multi-layer PCBs as the holes pass through all the holes it could be useful if the component is connected to all the layers which is a mere special case. The soldering method is also a time consuming method compared to that of the surface mount components.

2.2.1.2 Surface Mount Technology (SMT)

Surface Mount Technology are components, also called surface mount devices (SMD), that are placed directly on the surface of an electronic PCB circuit. These devices have tiny metallic pins close to the surface of the components. By using soldering paste it is possible to solder these tiny legs on the PCB. Many electronic components are offered in two versions one for the through-hole technology and another for the surface mount technology. In many PCBs the two technology are used in the same board to combine the advantages of each one also some parts are hard to be done in a surface mount technology. Normally surface mount components (SMC) are much smaller than those of the TH-Technology because they have either smaller leads or no leads. The dense capabilities of PCB with SMCs is much higher than those with THT. They are also easier to mount on PCBs which allows auto mounting with robots or machines. Also PCBs can have components on both ends which will double the density that a board can have but will make the routing area smaller. They also have lower inductance and resistance at the solder area as they are much smaller compared to those of the THT [21].

Figure 2-7 SMT Photodiode [22]

SMT drawbacks include prototype and assembly are difficult and requires high skill and special equipment because the soldering area is small also because components are near each other which make removing a component a huge problem. SMC cannot be placed on a bread board they are not easily tested. In addition in power circuits SMT is not an option as they are physically big components and they need better fixation on the circuit boards as well as the high temperature in these power circuits can damage the solder pads. Also as previously mentioned they cannot withstand mechanical stress compared to the through-hole technology [23].

This technology is useful in making a large number of photodiodes in a printed circuit which will increase the resolution of the sensor during solar tracking giving more accurate results. This sensor was chosen to be used in the hemispherical prototype eye. It also has a responsivity angle of 35 degrees, which is better than the THT photodiode as there will be less overlapping between the sensors.

2.2.2 Phototransistors

Figure 2-8 Phototransistor [24]

Phototransistors are transistors assembled in a transparent package, designed to capture light. Its advantage over the Photodiode is having built-in gain; absorbed light creates a current in the base region of the phototransistor, resulting in current gains from 100 to several thousands. A special type is photodarlington, which have two stages of gain with net gains reaching 100,000 and greater. The built in gain allows the phototransistor to be coupled with a load resistor to accommodate TTL level voltages for a wide range of light levels. Because of their ease of use, low cost and TTL compatible signal levels, phototransistors have become popular for applications where there is more than a few hundred nano-watts of available optical power. These devices however, do have some drawbacks compared to Photodiodes. The frequency bandwidth and linearity are relatively limited and spectral response is restricted to between 350 and 1100 nm. In addition, there are very large variations in sensitivity between individual devices and few standard package options. [18]

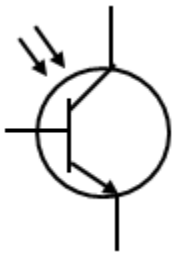

Figure 2-9 Phototransistor schematic

2.2.3 Photoconductive sensors

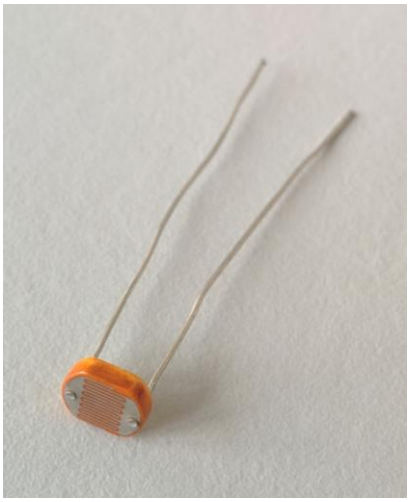

Figure 2-10 Photoconductive sensor

A photoconductive sensor is a thick film semiconductor material, with increasing incident light, its electrical resistance decreases [15]. These rough assemblies that can withstand hundreds of volts are usually less than 1 cm diameter. Due to the absorption of electromagnetic radiation such as visible light, infrared light, ultraviolet light, or gamma radiation, the photoconductive light sensor material becomes more electrically conductive. Photoconductive cells consist of a thin polycrystalline or single-crystal film of compound semiconductor substances.

The sensors based on cadmium sulfide (CdS) have sensitivity curves closely matching that of the human eye. Therefore, they are useful in applications concerning human light perception such as headlight dimmers and intensity adjustments on information displays. Photoconductive sensors can be designed for measuring microwatts to mill-watts of optical power and are very cheap at high volume. These features make CdS photoconductors the chosen sensor in applications such as street light control and in the toy industry where economy is a major consideration.

However, there are some considerations that limit the use of CdS in more sophisticated applications requiring sensitivities over small variations between individual parts, a wide spectral range, or no history-dependent response. [15]

Depending on the thick film microstructure, the resistance of these sensors changes, so the resistance specification has a wide tolerance - a max/min ratio of 3 is not uncommon. The resistance also has "long term memory" which depends, at any given time, on the amount of light actually incident on the sensor plus the sensor light history for the past several days.

Photoconductors made from materials other than CdS such as lead telluride and mercury cadmium telluride are also available. These materials have spectral sensitivities that cover the range that Photodiodes cannot: above 2 m out to 15 m. This longer wavelength sensitivity is very important for infrared imaging cameras and for long wave instrumentation such as is used to monitor carbon

dioxide laser emission and atmospheric physics. These sensors tend to be more expensive than both silicon Photodiodes and CdS photoconductors.

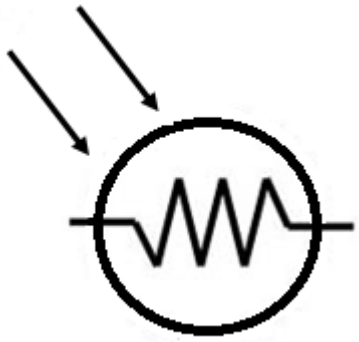

Figure 2-11 Photoconductive sensor schematic

2.2.4 Photomultiplier tubes

Figure 2-12 Photomultiplier tube (dia. 25 mm) [16]

Photomultiplier tubes are vacuum tubes that have a light sensing surface (the photocathode) this photocathode absorbs incoming light photons and releases secondary electrons. These secondary electrons are accelerated and multiplied within the photomultiplier tube by dynode plates. When an electron strikes a dynode at each time, it gains enough momentum to create a larger number of secondary electrons.

This multiplication process continues for each dynode within the tube. Tubes with ten to twelve dynodes can easily generate multiplications of more than a million, resulting in sufficient current to develop hundreds of mill-volts across an output 50 Ω load resistor for a single incident photon.

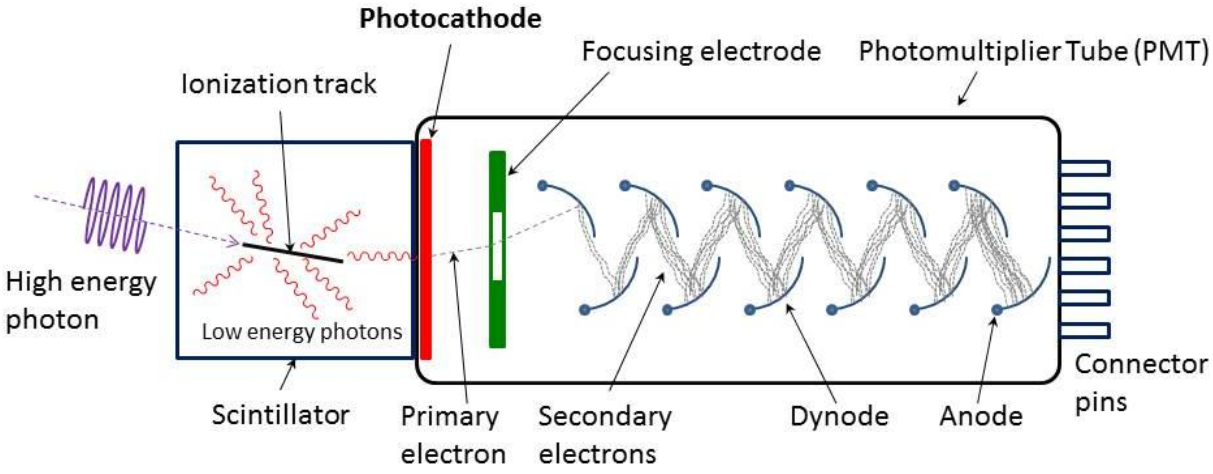

Figure 2-13 Photomultiplier tube schematic [16]

The combination of high gain, low noise, high frequency response or, equivalently, ultra-fast response, and large area of collection has earned photomultipliers an essential place in nuclear and particle physics, astronomy, medical diagnostics including blood tests, medical imaging, motion picture film scanning (telecine), radar jamming, and high-end image scanners known as drum scanners. Elements of photomultiplier technology, when integrated differently, are the basis of night vision devices. [16]

2.2.5 LED as detectors

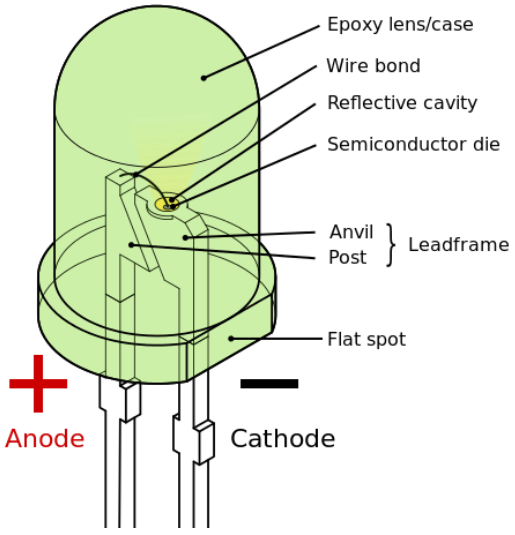

Figure 2-14 LED structure [25]

LED (light emitting diode) is a two-lead semiconductor light source. It is a basic pn-junction diode, which emits light when activated. Even though LEDs are mostly used as light sources,

they can be used for light detection. When light illuminates the emitting chip of an LED, small amount of current (~nA level) can be produced. An operational amplifier then has to be used to amplify the current to be read. Compared to other light transducers like Photodiodes, a LED is known to be more sensitive to the same wavelength which the LED emits. [25]

Figure 2-15 shows the available wavelengths of LEDs. Every one diode has certain range of light that it can sense more sensitively than a photodiode, but its range is very small to detect solar radiation, several LEDs with different spectral range have to be used which might not be suitable for the application in this thesis.

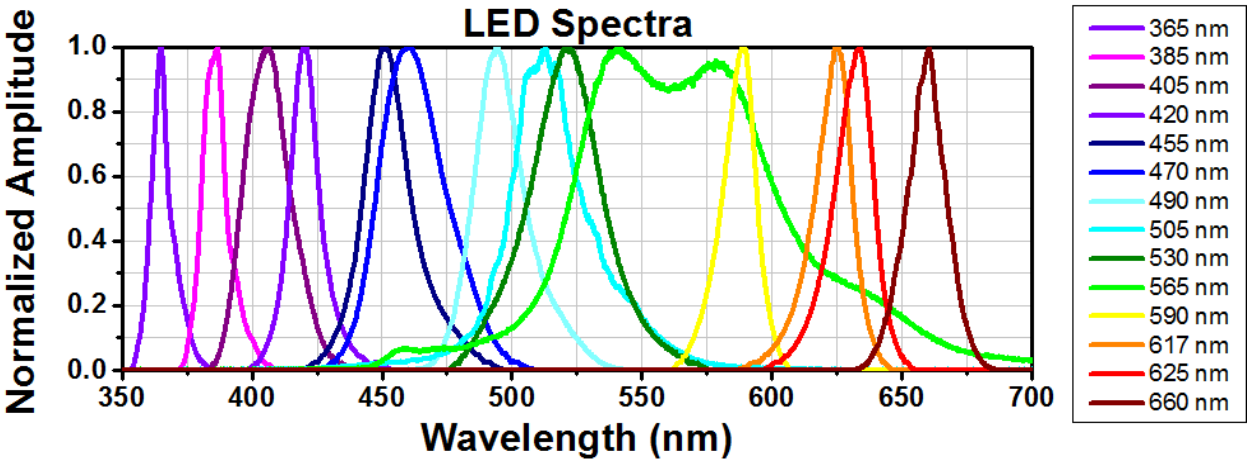

Figure 2-15 LED wavelengths [26]

2.3 Microcontrollers

A microcontroller is a solitary chip microcomputer fabricated from VLSI (Very Large Scale Integration) fabrication. It is also known as embedded controller. Various types of microcontrollers are available on the market with different word lengths such as 4 bit, 8 bit, 64 bit and 128 bit. It has the ability to control embedded system functions such as office machines, robots, home appliances, motor vehicles, and a number of other gadgets. A microcontroller comprises components like memory, peripherals and most importantly a processor. They are basically employed in devices that need a degree of control to be applied by the user of the device.

2.4 Multiplexing

Multiplexing is sending multiple signals to a medium at the same time and then recovering the each individual signal at the receiving end. Multiplexing is a common networking method that integrates multiple analog and digital signals into a signal transmitted over a shared carrier. Multiplexers and de-multiplexers are generally used to get one signal at a time from various signals. It is also known as muxing. Signal types can be analog or digital. It is used for transmission over a single line or media. A general type of multiplexing technique would take several low-speed signals to

be delivered by a single high-speed connection. This sharing is done by a device name multiplexer (MUX) that organizes the sent signals. Also another device called de-multiplexer (DEMUX) at the other end separates the signals again.

There are different methods of multiplexing. The two main forms of multiplexing is Frequency Division Multiplexing (FDM) and Time Division Multiplexing (TDM). Time Division Multiplexing (TDM) is divided to another two branches Synchronous and Asynchronous as shown in figure 2-16 [27].

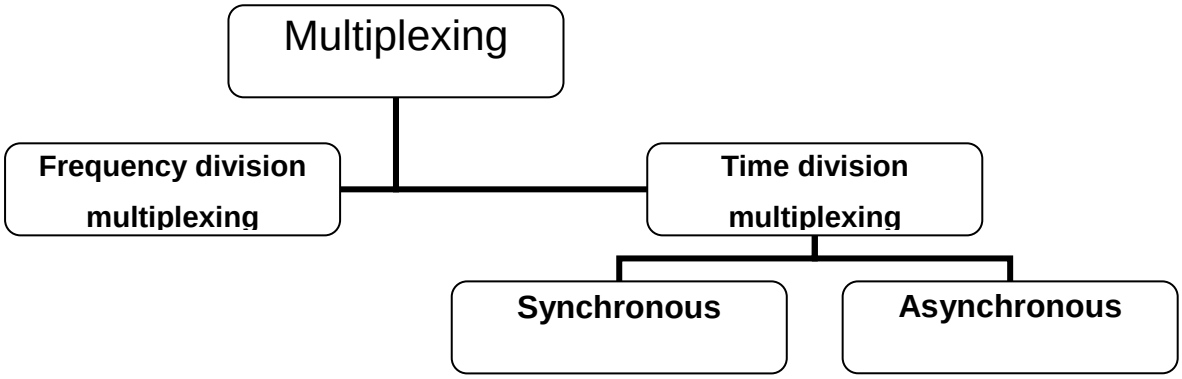

Figure 2-16 Multiplexing Hierarchy

Frequency Division Multiplexing (FDM) is considered as an analog technology. Frequency Division Multiplexing combines many signals to one connection by sending signals in multiple distinct frequency ranges over the single connection line. In order to the frequency division multiplexing method to work properly frequency overlap has to be avoided. Hence, the medium must have sufficient bandwidth which can carry the wide range of frequencies used. In order to achieve that a total bandwidth greater than the combined bandwidth of the signals to be carried to the other end. Also some strips of frequency that separate the signals which are called guard bands must be taken into consideration. At the receiving end, the de-multiplexer works by dividing the signals by tuning into the appropriate frequency.

One Example to illustrate could be the radio which operates in a similar way to FDM where a many different stations broadcast at the same time however each on distinct frequency. Listeners tune the radio channel to match the station they want to listen to [28].

Time Division Multiplexing (TDM) functions as follows. First, collecting and storing the coming signals from all the slow lines connected to it and giving a time difference on the faster connection to each transmission in its turn. The messages are sent down the high speed link one after the other. Each signal after being received can be detected again according to the time difference allocated. TDM is about sequencing groups of signals from an input stream, with a certain order. It requires the medium transferring the signals to be much faster than the individual receivers. The speed of the fast connector is equal to the sum of all the slow speed lines inputted to the multiplexer. Thus receiving devices will not be able to detect that the circuit was serving another communication circuit.

Synchronous Time Division Multiplexing works as follows, the multiplexer allocates exactly the same amount of time to each input it has. This time period is given whether the input is transmitting a signal or not. This is wasteful in that there will be some slice of times allocated which are not being used. This is the main drawback of this system. Therefore, the use of Synchronous TDM does not always produce maximum line usage and efficiency. On the other hand, In Asynchronous Time Division Multiplexing the slice of time given to each input is not fixed. Time is given only to inputs that have some data to transmit. Each input is given an Identification Number (IN) so that when it transmits data the receiving end would recognize the input and hence select the correct output. It requires more processing but saves overall time and reach maximum efficiency.

2.5 Flexible circuits

A Flexible circuit is a normal PCB but it has a special feature it can be bent and can take almost any shape. There are special components which are also flexible which can also be mounted on the flexible circuit resulting in a total flexible device. Also rigid normal components can be placed on top of the flexible circuit. The material in which these boards are made of differ from one manufacturer to another. However most of them use plastic substrates or a conductive transparent polyester. Devices can contain normal rigid printed circuit board and flexible circuit board. [29]

One of the advantages of the flexible circuits is it is thin which gives it the flexibility. This thin feature gives a possibility for a more integrated design and increasing the density of packages. Flex circuits are used in many application such as smart phones, sensors, LCD televisions, laptops ...etc. There is also a single layer flexible circuit as well as double layer and multilayer flexible circuit board. The only difference between the flexible circuit board and the normal rigid printed circuit board is the material of the routes, pads and vias.

Flexible circuits will be useful to be able to shape the sensor circuit into any shape needed, in this case a hemi-spherical shaped eye.

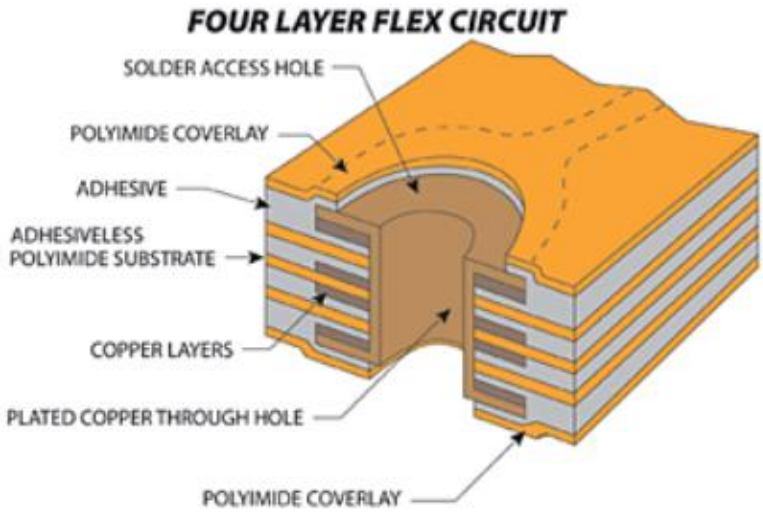

Figure 2-17 Flexible circuit illustration [30]

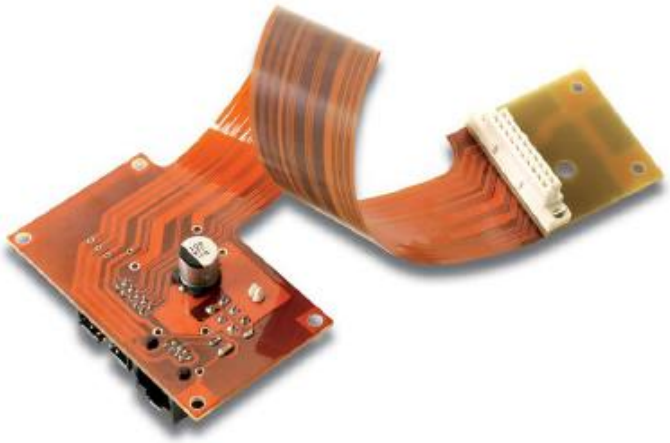

Figure 2-18 Flexible circuit [31]

2.6 3D printing

There are three main steps in creating parts or shapes using 3D printing: Modeling, printing and finishing. First modeling a CAD (Computer Aided Design) program is used to first create the part and then converted to a .STL (stereo lithography) file to be read by the 3D printer.

There are many ways of realize the model objects created by the 3D printers. One method use melting or softening material to put the layers on top of each other. Two of the most used technologies are fused deposition modeling (FDM) and Selective laser sintering (SLS). Laying liquid materials that are cured afterwards is another method of printing. The technology with this method is stereo lithography (SLA).

Ultimaker 2 is the 3D printer used in this thesis it uses the fused filament fabrication technique to build the layers to shape the final 3D product. It has a print speed and Travel speed of 30 mm/s to 300 mm/s. Its precision is 12.5 - 12.5 - 5 microns in width, length and height respectively. The layer resolution is 20 microns, the maximum build volume is 223 x 223 x 205 mm in width, length and height respectively. It was sufficient to build and test the prototype also to build the final eye. [32]

Figure 2-19 Ultimaker 2 3D printer

2.7 Solar Irradiance

The solar irradiance is the power per unit area reaching a surface, it is in the form of electromagnetic radiation. After atmospheric absorption and scattering, irradiance may be measured in space or at the earth's surface. The irradiance incident on the Earth's upper atmosphere is called the extraterrestrial irradiance (TSI). Irradiance is a function of distance from the sun, cross-cycle changes, and the solar cycle [33].

The energy in solar irradiance comes in the form of electromagnetic waves of a wide spectrum. The shorter wave lengths such as visible light or UV have more energy than longer wavelengths such as infrared. The spectral distribution graph (figure 2-20) shows the spectrum, the relative weights of individual wavelengths is plotted over all wavelengths, measured in W/m^2 (wavelength). Just outside the entry into the earth’s atmosphere, the diagram displays the spectrum of a sun ray. In the visible spectrum, the peak of the spectrum is found, but there are shorter and longer wavelengths with significant amounts of energy. [7]

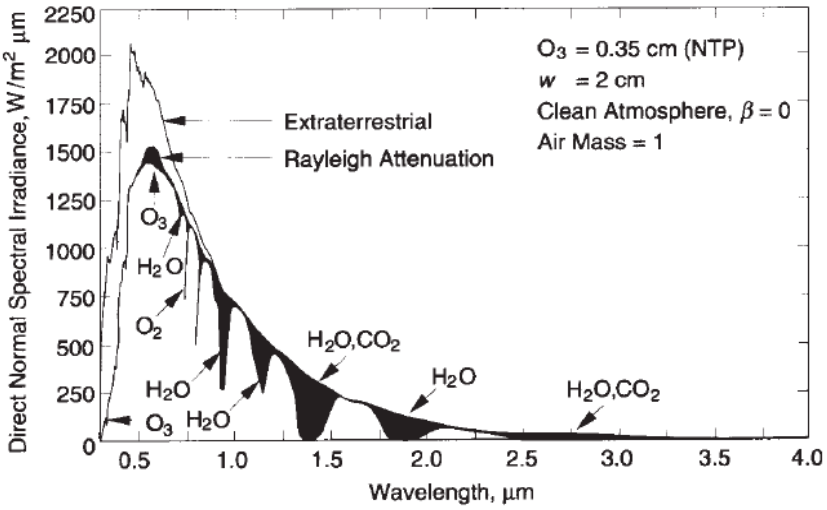

Figure 2-20 Solar spectral irradiance curve [7]

When the surface is perpendicular to the sun, irradiance is largest. As this angle moves from the right angle position, irradiance is reduced proportionally to the cosine of the angle.

As described by the horizontal coordinate system, the angle measured from directly overhead to the sun's center is called the zenith angle. The elevation (attitude) angle is the angle between the sun's center and the horizon. The azimuth angle is the angle measured from the south as shown by figure 2-21.

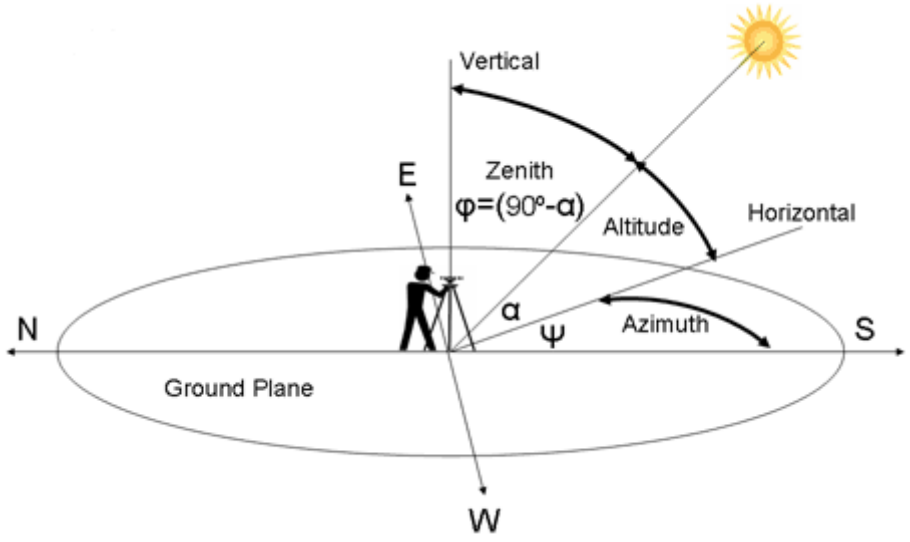

Figure 2-21 Zenith, elevation and azimuth angles [34]

If the zenith angle is not zero, for horizontal surfaces, a larger area is required to catch the same irradiance of a surface normal to the sunbeam.

Some definitions to differentiate between different kinds of radiation [7]

Beam Radiation It is the solar radiation from the sun without being scattered by the atmosphere. (Beam radiation is often referred to as direct solar radiation).

Diffuse Radiation It is the solar radiation from the sun after being scattered by the atmosphere.

Total Solar Radiation It is the sum of the diffuse and the beam solar radiation on a surface.

2.8 Solar Cells

A solar cell is a device that converts the solar energy into electricity by the photovoltaic effect. Characteristics such as current, voltage, or resistance, vary according to the irradiance of the sun on earth. They are the building blocks of photovoltaic modules, known as solar panels.

Electrical properties of devices are describe by current-voltage characteristics. It is useful to understand the origin of these current-voltage characteristics in terms of basic physical processes. The electronic functions of solar cells take place within materials called semiconductors. Semiconductors have the capacity to absorb light and to deliver a portion of the energy of the absorbed photons to carriers of electrical current – electrons and holes.

The conductivity of the semiconductors can be controlled (modified) through the introduction of specific impurities, or dopants called donors and acceptors. N-type (electrons are the majority carriers of electrical current). Obtained introducing donor impurities into a semiconductor. P-type (holes are the majority carriers of electrical current). Obtained introducing acceptor impurities into a semiconductor. [35]

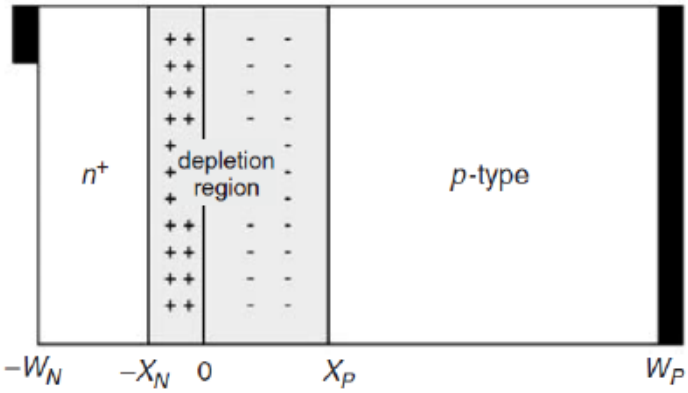

Figure 2-22 p-n junction [35]

Simple solar cell structure with the metallurgical junction at x=0 (figure 2-22). The fixed charges in the depletion region are due to ionized donors on the n-side and ionized acceptors on the p-side. There is a concentration difference of holes and electrons between the two types of semiconductors. Consequently, holes diffuse from the p-type region into the n-type region and, similarly, electrons from the n-type material diffuse into the p-type region. Consequently, an electric field (electrostatic potential difference) is produced which counteracts the diffusion of the holes and electrons. In thermal equilibrium, the diffusion and drift currents for each carrier type exactly balance. There is no net current flow and the Fermi energy must be independent of position: the Fermi level is continuous throughout the crystal. Space-charge region or depletion region: transition region between the n-type and the p-type semiconductors. This region is depleted of both electrons and holes. Neutral region: charge-neutral regions on either side of the depletion region built-in voltage, Vbi, electrostatic potential difference resulting from the junction formation.

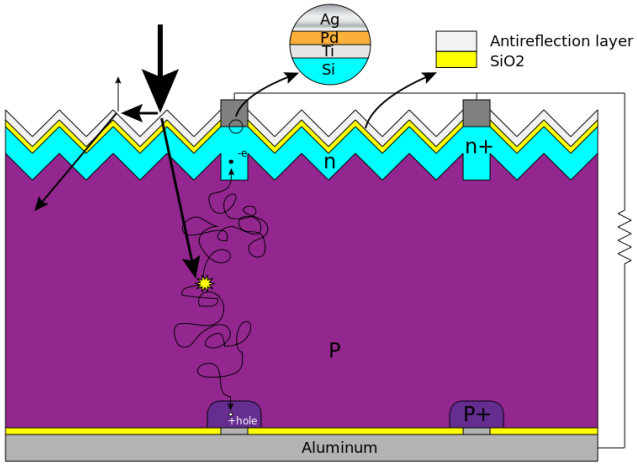

Figure 2-23 Working mechanism of a solar cell [17]

A solar cell is simply a p-n junction diode basic structure with emitter region which is the more heavily doped quasi-neutral region. A base or absorber region which is the more lightly doped quasi-neutral region.

The ideal current-voltage characteristics are based on the following assumptions: The abrupt depletion-layer approximation; that is, the built-in potential and applied voltages are supported by a dipole layer with abrupt boundaries, and outside the boundaries the semiconductor is assumed to be neutral. The Boltzmann approximation is valid. The low-injection assumption; that is, the injected minority-carrier densities are small compared with the majority-carrier densities. No generation-recombination current exists inside the depletion layer, and the electron and hole currents are constant throughout the depletion layer.

For the solar cell to operate, photons hit the solar cell, electrons are excited from their current molecular/atomic energy level to a higher level. They can either dissipate the energy as heat and

return to the original level or travel through the cell until it reaches an electrode. Therefore a DC current flows through the material and the electrodes. [35]

The short-circuit current, I_{SC}, and dark saturation currents, I_{01} and I_{02} depend on the solar cell structure, material properties, and the operating conditions. These quantities are given by rather complex expressions. A solar cell can be modeled by an ideal current source – I_{SC} in parallel with two diodes – one with an ideality factor of 1 and the other with an ideality factor of 2:

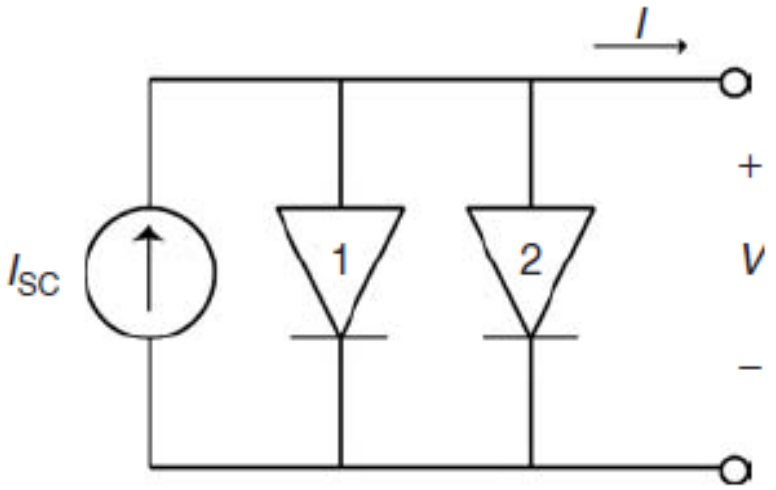

Figure 2-24 Simple solar cell circuit model [35]

The current-voltage I(V) characteristic of a typical silicon solar cell is shown by figure 2-25.

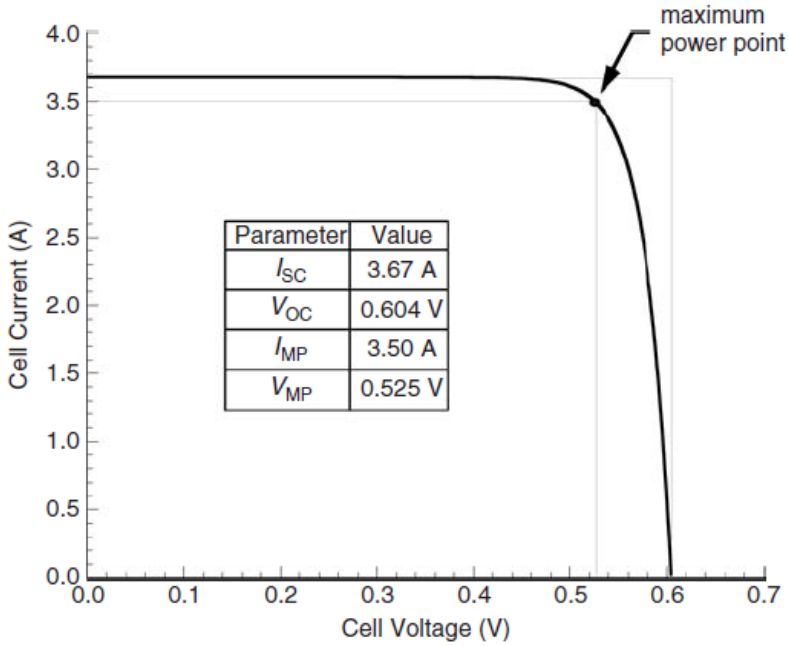

Figure 2-25 I-V characteristic curve [35]

The important terms for solar cells: the short circuit-current, I_{SC}, the open-circuit voltage, V_{OC}, the fill factor, FF, and the cell efficiency, η. At small applied voltages (V ≈ 0), the diode current is negligible and the current is just the short-circuit current, I_{SC}. At high applied voltages, the diode currents becomes significant, and the solar cell current drops quickly. At open-circuit (I = 0), all the light-generated current I_{SC} is flowing through diode 1 (diode 2 ignored)

$$V_{OC} = \frac{kT}{q} \ln \frac{I_{SC} + I_{01}}{I_{01}} \approx \frac{kT}{q} \ln \frac{I_{SC}}{I_{01}} \tag{4}$$

Where $I_{SC} >> I_{01}$

Maximum power output point (MPP) on the I(V) curve is where the power produced at a maximum: V = V_{MP} and I = I_{MP}. These point defines a rectangle whose area, given by $P_{MP} = V_{MP} * I_{MP}$, is the largest rectangle for any point on the I(V) curve.

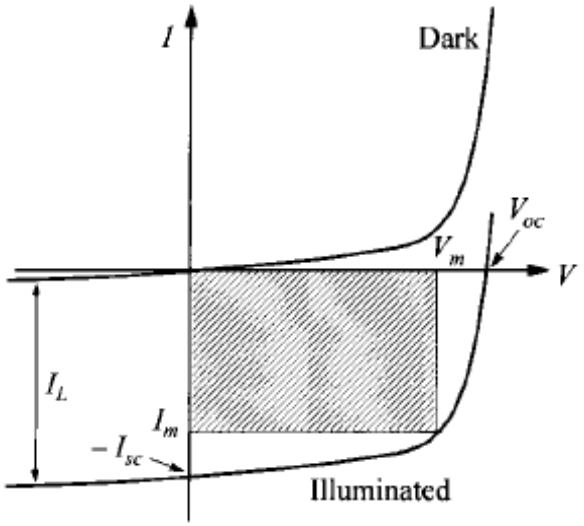

Figure 2-26 I-V characteristics of solar cell under illumination. Determination of maximum power output is indicated. [35]

The rectangle defined by V_{OC} and I_{SC} provides a reference for describing the maximum power point. The fill factor, FF, is a measure of the square-ness of the I-V characteristics and is always less than one. It is the ratio of the areas V_{MP}, I_{MP} and $V_{OC}*I_{SC}$.

$$FF = \frac{V_{MP} I_{MP}}{V_{OC} I_{SC}} = \frac{P_{MP}}{V_{OC} I_{SC}} \tag{5}$$

The power conversion efficiency, η, is the most important figure of a solar cell, which is defined as

$$\eta = \frac{P_{MP}}{P_{in}} = \frac{FFV_{OC}I_{SC}}{P_{in}} \tag{6}$$

Where P_{in} is the incident power. [35]

A solar photovoltaic panel or module is made from multiple solar cells in parallel and series connections as shown in figure 2-27. Photovoltaic panels often have a sheet of glass on the sun-facing side, allowing light to pass and protecting the semiconductor wafers. When solar cells are connected in series in modules, the voltage is added. Connecting cells in parallel, the current is added; however, problems such as shadow effects can shut down the less illuminated parallel string (series connected cells) causing power loss and possible damage because of the reverse bias applied to the shadowed cells by their illuminated partners.

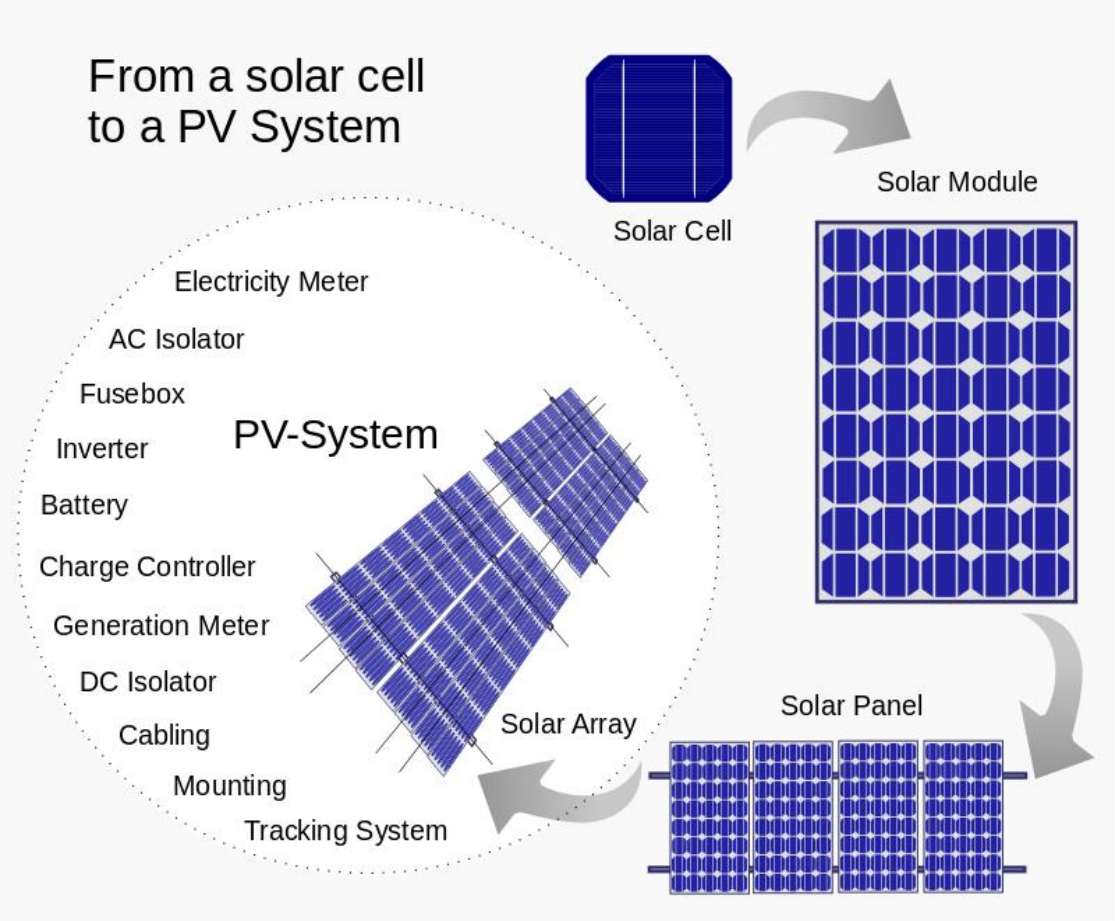

Figure 2-27 From a solar cell to a Photovoltaic system [36]

Chapter 3

Experimental setup and sensor design

This chapter presents the mechanical setup of the solar tracker and the creation of the hemi-spherical sensor for solar irradiation detection.

3.1 Mechanical design

It was required to move the solar panel to the angle of maximum irradiance that is detected by the insect eye. The implementation of the moving mechanism will allow the solar panel to follow the light. The proposed moving mechanism is a 2 degree of freedom mechanism that can rotate about two axis. The structure implemented satisfying the 2 degrees of freedom requirement for solar tracking is the rotate and tilt mechanism shown by figure 3-1.

The motors used for this implementation are servo motors. Servo motors are rotary actuators that have their own built in control circuit. This control circuit makes it possible to choose the exact location of the end position of the motor axis. Also, some servo motors can control the velocity instead of the position, and others can control the acceleration of the actuator, however, only one attribute can be controlled at a moment. The internal circuitry of the servo motor uses closed loop servomechanism feedback to reach the desired position, velocity or acceleration [37]. The motor chosen for this mechanism is a position control servo motor. It rotates 360 degrees, has a high torque of 120 Ncm torque at 6 volts and weighs 62.5 grams. Two of these motors were used to achieve the 2 degrees of freedom required.

Arduino Mega 2560 is the controller used to control the movement and also used to get the reading from the photodiodes (sensors). The moving mechanism was first designed using Solidworks. Then a simulation using Solidworks Motion was performed to insure that the motion capabilities were free from collisions. The 3D printer Ultimaker 2 was used to create the connecting link between the two servo motors as shown in the following figure 3-1.

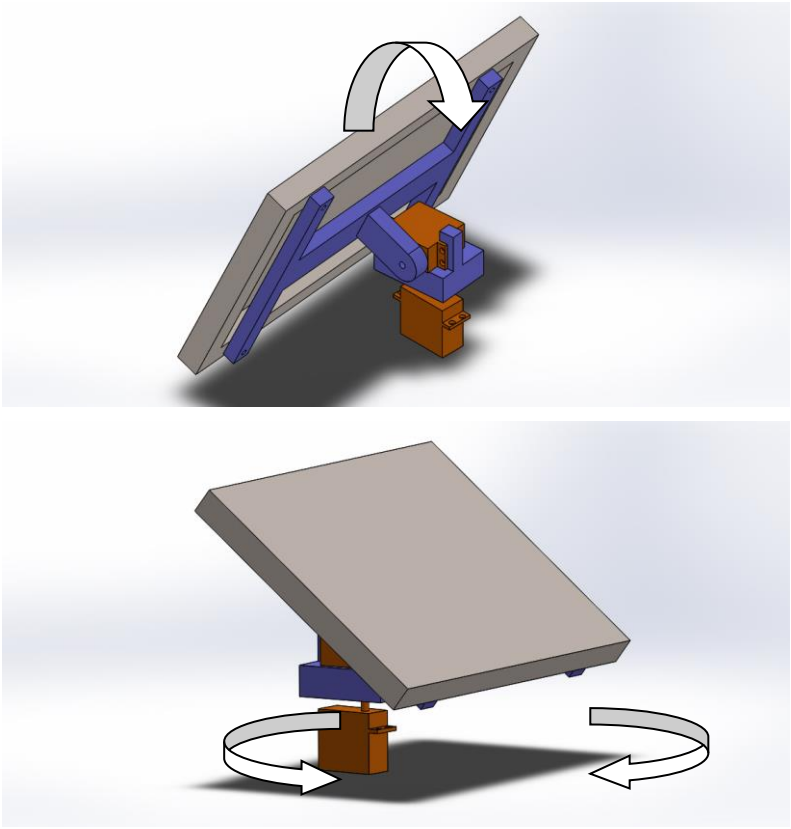

Figure 3-1 Moving mechanism

Figure 3-2 Real moving mechanism

Furthermore, an I-shaped part was made to hold the solar panel as shown in the previous figure. The motor's output torque was enough to hold the system as parts made from the 3D printer were light in weight, each of them is in the range of 70 grams. Since the servo motors do not need any driving circuit as their own circuitry is already build in makes them compact and easy to use. Also, there is a build in library in the Arduino to control servo motors. Refer to the annex A.1 for the schematic of the 2 parts made by the 3D printer.

The mechanism is tested with the Arduino to check its capability and to make sure it can be used for solar tracking.

3.2 Multiplexing circuit

This section presents the design of the multiplexer circuit used to rotate on all photodiodes of the eye and read their values.

Eagle is a software used to produce schematics and circuit board designs. This circuit was designed to take in 96 signals or photodiodes in this case and output 3 signals to be read by the Arduino. As discussed in the previous chapter, multiplexing the method used in this prototype is Time Division Multiplexing.

To be able to achieve the 96 to 3 multiplexer effect in this circuit, 6 multiplexers of 16 to 1 were used and three 2 to 1 multiplexers. Also, 96 resistors, which were used to make a voltage difference to be measured by the Arduino, were placed in this circuit. The value of these resistors can control the sensitivity of the sensors. The value of each resistor was 1 MΩ. In addition this circuit also had 2 pin headers each with 50 pins. These 100 pins were used to take signals from the sensor where 96 are sensor inputs and the other 4 are output or +5 V supply to the sensors. Also, two 100 nF capacitors were connected to the VCC of each IC.

Another pin header with 10 pins was used as a connection to the Arduino to send the eye readings to the Arduino and receive the control signals from the Arduino. Three output signals to be connected to the analog inputs of the Arduino, 5 control signals as input to the multiplexer circuit to choose the correct bit to output and the remaining 2 are +5 V and GND required to any device.

The first component to be discussed is the 16 to 1 multiplexer. Some requirements were chosen first and then it was chosen based on these requirements. First of all, it had to be an analog multiplexer as digital multiplexers cannot be used because the output of the sensors is analog. Secondly, the working environment of the multiplexer should be compatible with both the Arduino and the sensors used. Finally, it was SMD technology not Through Hole Technology (THT) as it saves area.

Since 6 of these multiplexers were used, they had to be reliable, available and cheap. The 74HC4067 Texas Instrument 16 to 1 Analog multiplexer/de-multiplexer was chosen. It has a low ON resistance 70 Ω which was good as it did not affect the signal with noise. It works with +5 V so it was compatible with both the Arduino and the sensors used. It was a surface mount device and it had a

standard connection layout in PCB's, so it can be easily used in any software such as Eagle software. All propagation times was in the range of 80 ns which was good compared to the clock of the Arduino 16 MHz.

The second component is the 2 to 1 multiplexer. The same requirements were considered as for the previous one. The chosen multiplexer in this design was the CD74HC4053 Texas Instrument analog multiplexer. It had three 2 to 1 multiplexers so it was very compact and cheap. It also had low ON resistance of 70 Ω to reduce noise. It operates with +5 V, so it was compatible with the Arduino board. The propagation time was in the range of 40 ns, which makes an overall propagation time of about 120 ns. This value was considerably good with respect to the Arduino. It can work with up to 200 MHz. It was also a SMD and easy to use in software.

Furthermore, there were 96 resistors in total. SMD resistors have many standards, the difference between these standards is the dimension, the width and length. 0603 was the standard size used in this design, and as this number increases, the size of the component increases. Each of these resistors has a value of 1 MΩ. This standard was chosen because of its small size that fits to the circuit.

The schematic (found in annex A.2) shows the connections between the parts and the logic behind the whole circuit. As shown in the schematic, the 50 pin connectors had a strange arrangement, which seem random. This order was used according to the board layout (also shown in annex A.2). In order to have similar connections this order was chosen. This caused having an ambiguous code rather than having a complicated hardware.

In the board layout the blue lines refer to the bottom layer connection and the red lines refer to the top layer. The small circles are the vias and the bigger circles are the pads of the connectors. The outline of each component is also shown in the design. There are two big circles which are holes for fixing the multiplexing circuit. The dimension of this circuit is 75 x 75 mm. The width of each track - blue and red line - is 10 mm. The diameter of the vias is 0.5 mm.

The table for the connection to the multiplexer circuit board, as it was not done in order, can be found in annex A.3. The table maps the connections from top left to bottom right and moving row by row. Each row is represented as a column in the table. The term IC-No. is for IC is the number of the IC and the No. is the pin number in the IC. For example 6-01 this means it is connected to IC number 6 to pin number 1 in this IC. The pin column is for the pin of the connector.

To manufacture the circuit after the design has been made with Eagle software. Gerber files were extracted from Eagle. The standard used in extracting the gerber files is GERBER RS274X. Eight gerber files were extracted from the board layout. The sum of these gerber files is simply the layout in the annex. The first gerber file was the top copper, it has the top, pads, vias and dimension layers numbered 1, 17, 18 and 20, and its extension is .GTL. The second gerber file was the bottom copper, it has the bottom, pads, vias and dimension layers numbered 16, 17, 18 and 20, and its extension is .GBL. The third gerber file was the top silkscreen, it has the t-place and the t-names

layers numbered 21 and 25, and its extension is .GTO. The fourth gerber file was the top paste, it has the t-cream layer numbered 31, and its extension is .GTP. The fifth gerber file was the top solder-mask, it has the t-stop layer numbered 29, and its extension is .GTS. The sixth gerber file was the bottom solder-mask, it has the b-stop layer numbered 30, and its extension is .GBS. The seventh gerber file was the drill file, it has the dimension, drills and holes layers numbered 20, 44 and 45, and its extension is .TXT. The last gerber file was the mill layer, it has the dimension and milling layers numbered 20 and 46, and its extension is .GML.

The next step was to manufacture this PCB. After contacting some PCB manufacturing companies. Multi-CB Ltd. was chosen to produce all the PCBs that are used in this project including other circuits that will be discussed later. Three of these circuits were ordered, in addition to a stencil as this circuit had many components and most of them are small, so placing solder paste over all of these pads one by one would have been tedious and would have taken a lot of time. With a stencil it only took a few minutes to apply the solder paste on all the pads. The stencil machine used for fixing and putting the solder paste is called SD 240 SMT stencil printer. For more information on PCB circuit fabrication, please refer to annex A.4.

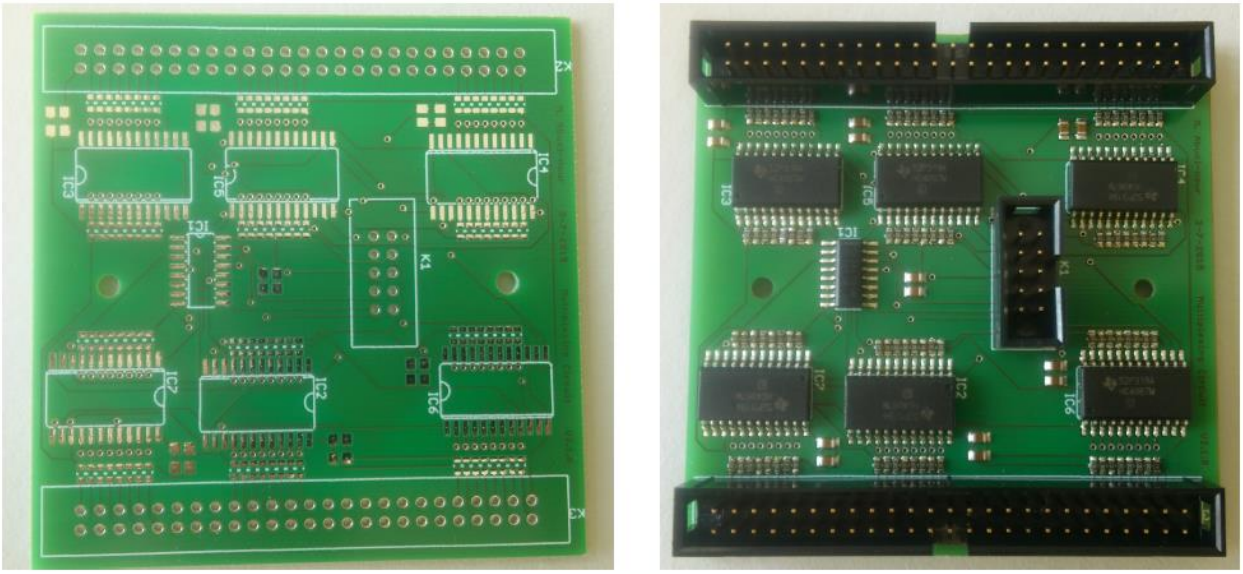

Figure 3-3 Multiplexer circuit before and after adding components

3.3 Photodiode

The photodiode used in this prototype was Vishay Semiconductors Vemd2503X01, an SMD photodiode. It has a small area, approximately one-fourth the THT photo diode. Its dimensions are 2.3 x 2.3 x 2.55 mm in length, width and height respectively (Figure 2-7). The detection wave length is from 350 nm up to 1120 nm, a good range for solar radiation detection. It has almost one forth the sensitive area of the THT diode, which is 0.23 mm^2. It has dark current has a maximum of 10 nA which is small and negligible. The reverse light current is typically 10 µA at a reverse voltage of 5 V.

The rise and fall time are 100 ns each. The most important feature is that it has a linear relationship between the irradiance and the reverse current at a reverse voltage of 5 V at normal temperature with small fluctuations when it is over 60 ^{o}C or less than 20 ^{o}C.

3.4 Hemispherical eye

Creating a spherical eye was a very challenging task as PCB's cannot normally be bent to take curves in 2 directions even if they are flexible PCB's. But, to produce a hemispherical eye that looks like a normal insect eye, it was required to bend a flat PCB to take the hemispherical shape. The idea began by making several paper stripes that were thin and bend them on a curved surface.

To test this idea, a hollow hemisphere was designed using Solidworks and then created using the 3D printer. Afterwards, Solidworks was used to make this design as shown in figure 3-4.

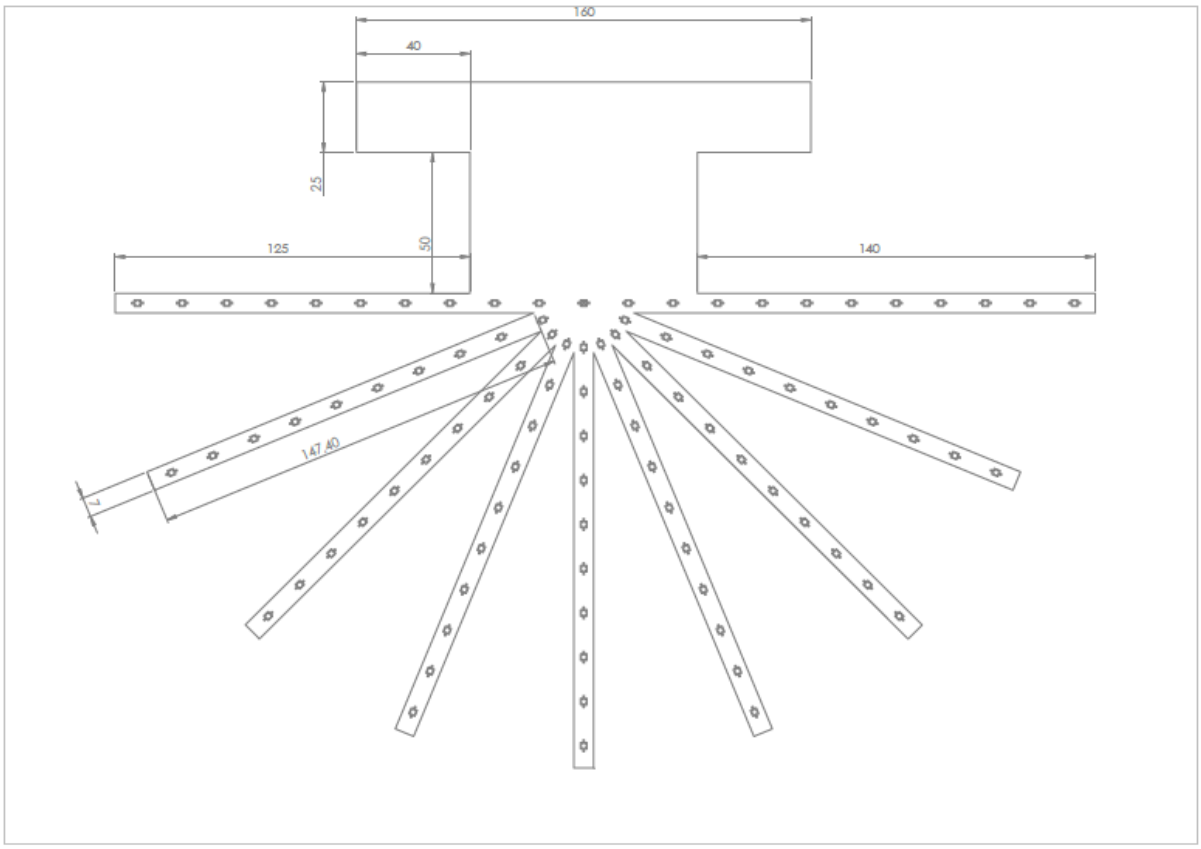

Figure 3-4 Sensor Stripes to be bent

The next step was to try this drawing after cutting it properly on the hemi-sphere created using the 3D printer. The design worked perfectly except that the stripes were moving freely and were not guided on the hemisphere, so guide paths for each stipe were made. This was also useful in having equal distances between the stripes so that the photodiodes are distributed exactly the way it

was intended to be in the design. Higher densities than the 92 photodiodes used can help in having a more accurate tracking, but for the purpose of a prototype, these 92 were enough. This hemispherical eye has photodiodes in all directions (can be seen in figures 3-6 and 3-7). Refer to annex A.1 for the hemispherical eye schematic.

Figure 3-5 Hemi-sphere paper trial

The most difficult step was to create a PCB with the same shape as figure 3-4. Also to connect them to the multiplexer circuit discussed in section 3.2. Eagle software was used to create this circuit board and its schematic. However, the board layout took many trials to achieve good connections, in most of the times, a connection is unsuccessful or a whole part is trapped in all directions. To create the borders of the PCB, the drawing of Solidworks was used to achieve both the coordinates of the vertices and the location of the photodiodes. Although the accuracy of Solidworks was much better than that of the Eagle software, the layout was achieved in Eagle. The stripes that were going to be bent on the spherical shape are the long thin rectangles.

There are 9 stripes, each having 10 photodiodes numbered from 1 to 10 starting from the top vertical strip, resulting in 90 photodiodes. The one in the middle is separate and its number is 91. The bottom vertical strip was a special strip as it had 11 photodiodes where eleventh diode will be on the opposite side of number 91, having the number 92. This results in 92 photodiodes. Moving in the anticlockwise direction in figure 3-4, we have photodiodes from 11 to 20 in the second strip, 21 to 30 in the third ...etc. Number 91 is the middle one and number 92 is the most bottom photodiode, the extra one in the special strip.

The PCB has two connectors each of 50 pins, 92 of them are for the photodiodes the other 8 are +5 V for the photodiodes. As in the previous PCB layout, the red line are for the top routes and the bottom routes are blue. The pads and vias are the circles in the layout. The smaller circles are the vias and they are scattered throughout the PCB. All vias have a diameter of 0.5 mm. Also the outline of the pin connectors is in grey as well as the location of each photo diode. The dimension of this

circuit is the same as the Solidworks drawing in figure 3-4.The route width is 10 mils for both top and bottom routes.

The table in annex A.3 presents the diode number versus its location in the pin connector. The first two columns are for the first connector and the other two are for the second connector. Also, schematics of the hemispherical circuits are shown in annex A.2.

To manufacture the circuit after the board layout is made, the gerber files are extracted and sent to the PCB manufacturing company Multi-CB Ltd., this PCB was relatively big (the size of an A3 paper), therefore this PCB was expensive. The whole prototype cost around 600 €.

3.5 Mapping and connecting the eye

Double face tape was used to attach the circuit to the 3D printed model. The eye was then fixed on a post and connected to the multiplexer circuit using 2 ribbon cables. The multiplexer circuit was connected to the Arduino using another smaller ribbon cable. The multiplexer circuit was fixed on a wooden plate where other circuitry and the solar panel mechanical setup are located.

Mapping the photodiodes was the most difficult part as the arrangement of the photodiode connections to the pic connectors is random and there is no pattern between the multiplexer circuit and the hemi-spherical eye circuit. After several trials the correct mapping is done by comparing both the pin connectors schematic in the eagle software and the orientation of the ribbon cables in reality. Furthermore MATLAB was used to preview the photo diode readings as a 2D array pixel image that shows the readings of the photodiodes, the higher the reading, the brighter the pixel is and the brightest pixel shows the maximum point of irradiance. The Arduino and MATLAB codes are found in annex B.

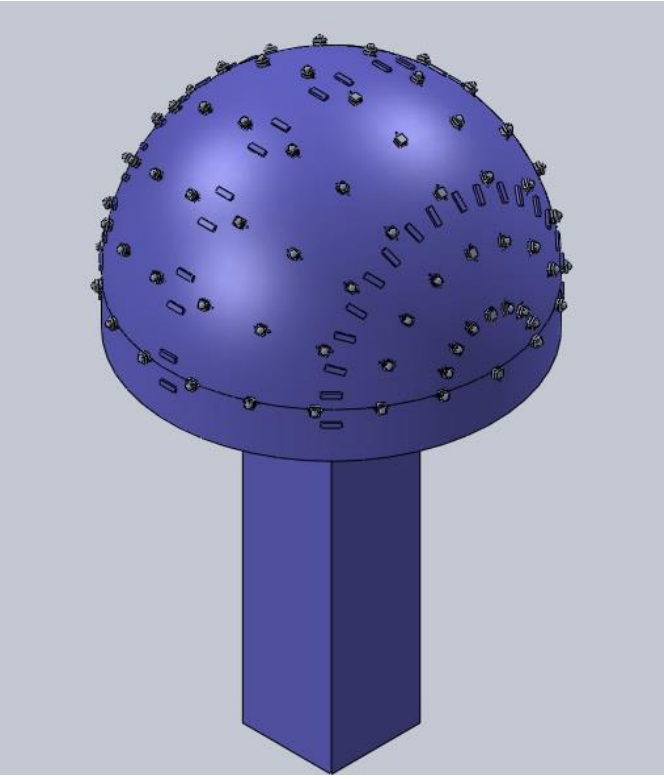

Figure 3-6 Solidworks view of the eye on a post

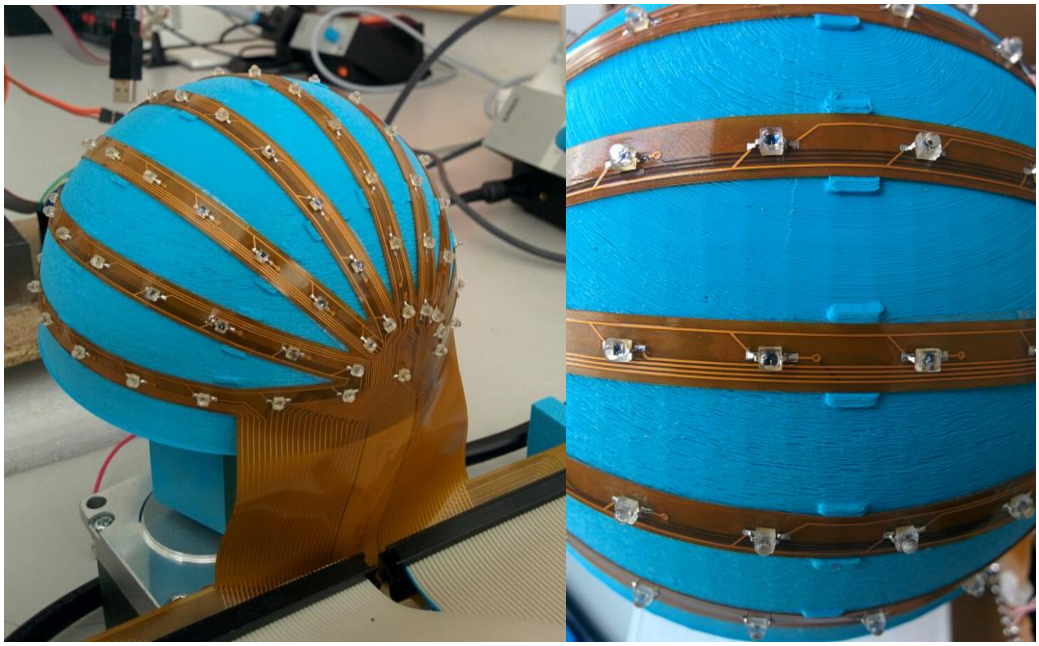

Figure 3-7 Real eye

Chapter 4

Results and Issues

4.1 Results

The Arduino Mega 2560 was the brain used in this project. The Arduino was used to interact with the multiplexer circuit to both send the controlling signal also to acquire the image from the sensors and sending the image to the computer to preview it. The Multiplexing circuit used was successful and was able to rotate on all photodiodes and send their values to the Arduino. It takes the 96 sensors and outputs only in 3 signals according to the selection lines. The concept of this circuit can be further used in achieving more pixels in the eye as the Arduino Mega can take up to 5 of these circuits working at the same time as it has 16 analog inputs.

The photodiode's response to light is noticeable and reliable. The response highly depends on the value of the resistance connected in series with it.

As for the hemispherical eye, several problems were faced during testing that are discussed in the following section. These problems resulted in changing the prototype to a previous prototype that was built for another purpose but can give reliable results as a prove of concept that the eye can be used to detect the maximum point of irradiance.

4.2 Problems and Issues

4.2.1 Connections

In order to connect the multiplexer circuit with the eye, ribbon cables are used. The problem was that the 50 wire ribbon cable is nearly rigid or not flexible enough, so the connection was not robust and not fixed well. Also the pin connectors used in this circuits were large, THT and had sharp edges that affected some tracks in the flexible circuit of the eye. The normal soldering techniques to solder these pads was not robust and was not connected well, so the photodiodes were not connected well to the multiplexer circuit.

After testing the eye for the first time, the diodes were working and the tracks were connected. After some experiments with the eye to be able to map the sensors correctly for visualization, some tracks and some pads were cut and stopped connecting due to the rigidity of the cables and poor soldering, they connected only when pressured by hand but give floating results, so it was very unreliable. One reason for this problem was the long neck of the eye carrying the 2 pin connectors and the other one was the edges of these connectors. Many approaches were used to solve this problem, such as re-soldering and externally connecting the photodiodes using normal wires. However, only the right-outer-pads could be solved, but the inner pads were not very

successful. Nearly about 40% of the photodiodes were not connected properly, some gave meaningless values (floating values), others had a very weak response to light and were barely noticeable and some diodes gave large values in no light conditions. Due to this problem, this eye was not useable for either trying to prove the concept of the thesis or integrating it with the mechanical setup to track the sun and of course cannot be compared to commercial sensors.

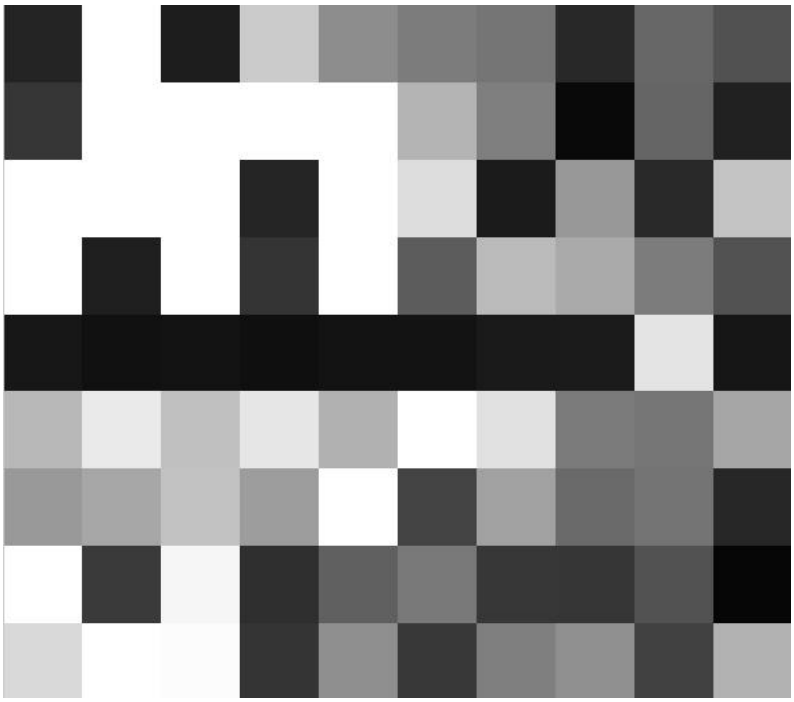

Figure 4-1 Hemi-spherical sensor preview

Figure 4-1 is the MATLAB image received by this faulty eye. The Arduino reads analog values ranging from 0 to 255, where 0 means that the photodiode is reading zero light intensity, and 255 means that the photodiode is reading maximum light intensity. White tiles represent the brightest pixels of the value 255 and black tiles represent the darkest pixels of the value 0, all values in between 0 and 255 were represented by the gray scale, the brighter the pixel, the more intensity it reads. As shown in the figure, several diodes gave the maximum value (white), and the middle strip showings no response to light at all (black), what can be understood from this image is that the light is coming from the left part of the sensor, but no exact location of the light can be given.

4.2.2 Sensitivity

In the multiplexer circuit, 1 MΩ resistance was used. The photodiode's sensitivity to light and radiation depends on this value. When the eye was put in direct sunlight, the image given was a white image with no variations which was due to the effect of bad connections and high sensitivity of the photodiodes due to large resistances.

4.3 Previous prototype results

To be able to have reasonable results and to prove the concept of this thesis, a previous prototype eye was used, which was built for the purpose of tracking the light indoors.

The eye is curved circularly in one direction and only slightly curved in the other. So it can only be used to track the sun in one axis, therefore it could not be integrated with the movement of the solar panel too, it would give inconsistent results. Also, it cannot be compared to other commercial sensors.

This eye had resistances of 1.5 MΩ, meaning that the photodiodes were very sensitive to light. To solve this problem a bread board was used and smaller value resistances were used to make it suitable for outdoor experimentation.

The previous prototype eye had a much smaller number of pixels (photodiodes) of 32 pixels, distributed 8 x 4 on the eye's surface. But, its circuit was handmade so the resistances can be changed, hence the sensitivity can be changed and tested. The sensor is presented in figures 4-2 and 4-3.

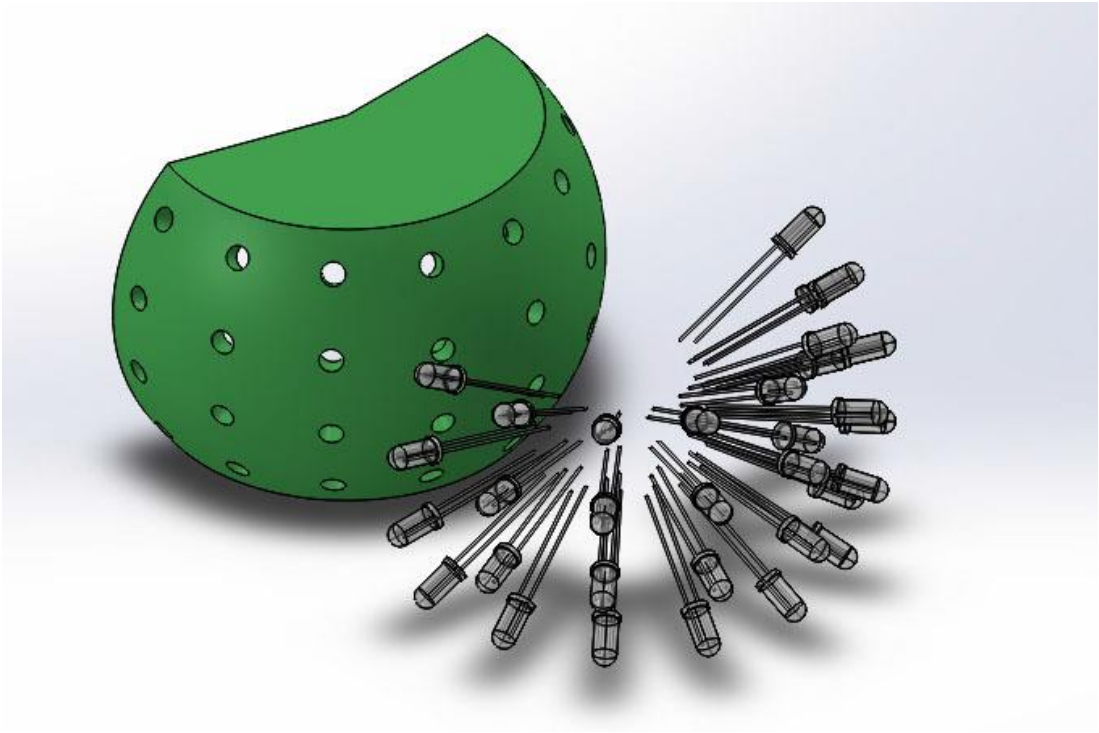

Figure 4-2 Exploded view of the previous prototype eye

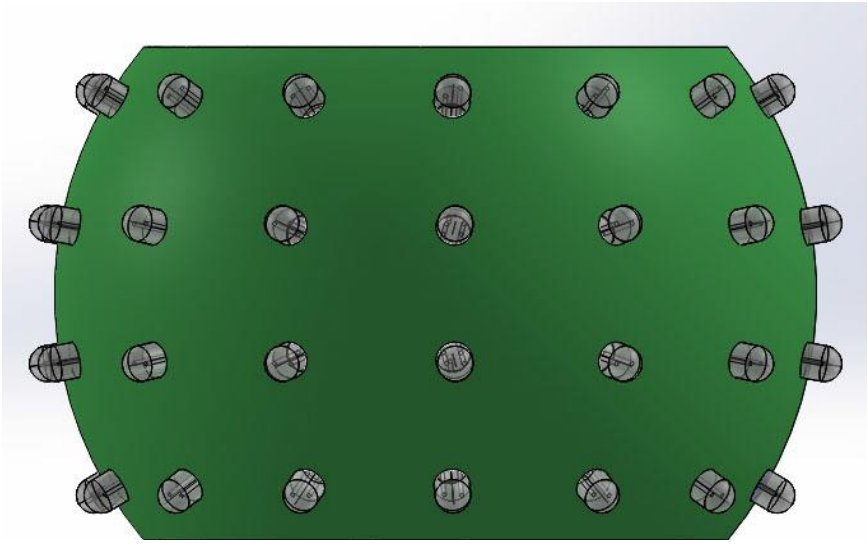

Figure 4-3 Top View

The best resistance used to achieve good readings in direct sun light with no clouds was the 5 kΩ which is much smaller than the resistance used in the multiplexer circuit. In cloudy conditions or partially cloudy conditions, a 50 kΩ resistance is used to have good readings. Figure 4-4 shows the results on a sunny day while using different resistances each time for the same orientation and position of the sensor in the field. The values used are 50 kΩ, 20 kΩ, 10 kΩ and 5 kΩ, starting from upper left to bottom right.

Figure 4-4 Effect of varying resistance during sunny conditions

As shown by figure 4-4, changing the resistance had a large effect on the sensor's sensitivity to irradiation coming from direct sunlight. The 50 kΩ was very sensitive during that time and many photodiodes have reached their maximum value, so pin-pointing where the sun is was not successful.

Going down to the 20 kΩ and 10 kΩ resistances gave more specific results about the location of maximum irradiation, but still more than one photo diode reached its maximum value.

When the 5 kΩ resistance was used, the maximum point of irradiation has been found out as shown in the bottom right image, and the solar panel was directed manually to that angle. The values of the solar panel power output was taken in the horizontal position and oriented position given by the eye. The solar panel's power rating is 5 W.

Solar panel's power in horizontal position: **3.76 W**

Solar panel's power when oriented according to the eye: **5.16 W**

So the sensor was successful in determining the maximum point of irradiance in sunny conditions.

However, in cloudy conditions, the 50 kΩ resistance worked best. Higher resistances than 50 kΩ were too sensitive and gave a white image, lower resistances were very non-sensitive and gave black images. Figure 4-5 shows the eye working with 100 kΩ, the eye has only been able to detect that the sun is on its upper right side. Figures 4-6 and 4-7 show the results in cloudy conditions with different orientation of the sensor.

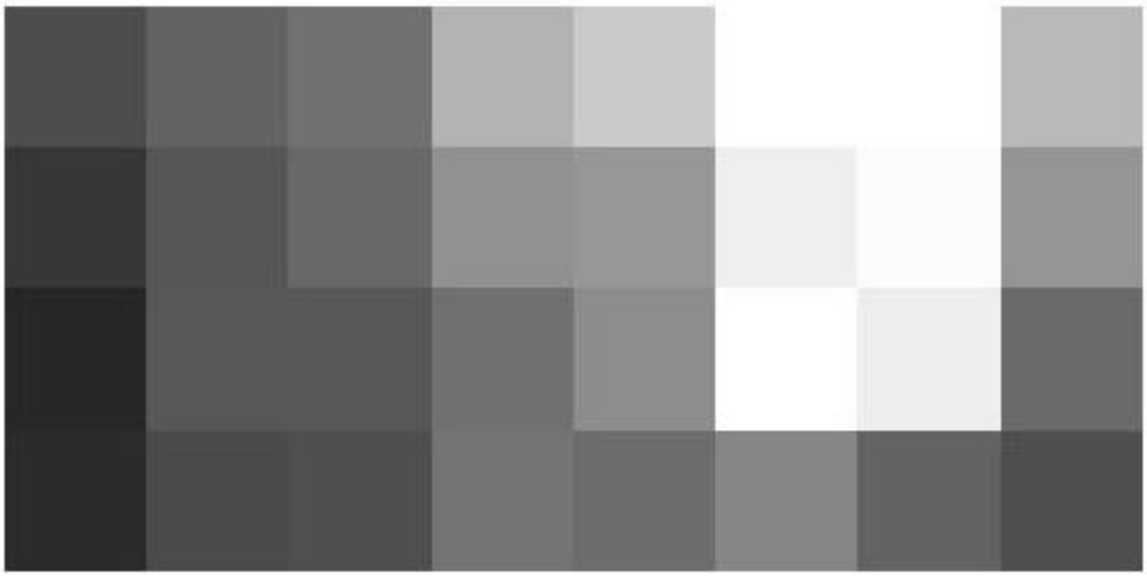

Figure 4-5 100 kΩ resistance results in cloudy conditions

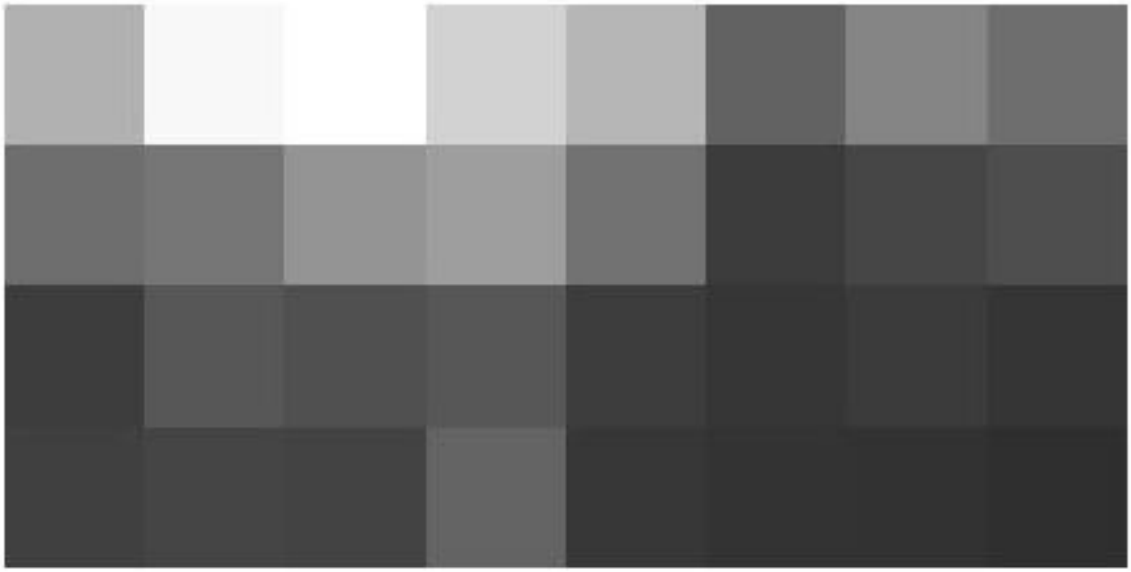

Figure 4-6 50 kΩ resistance results in cloudy conditions

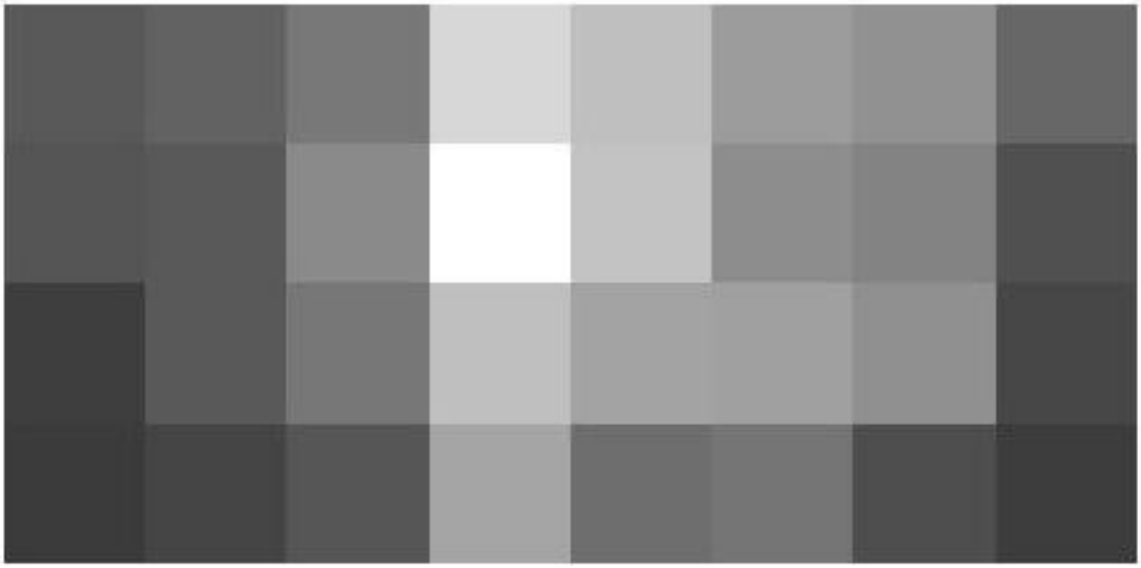

Figure 4-7 50 kΩ resistance results in cloudy conditions with different eye orientation

As shown by the previous figures, the sensor is able to detect the point of maximum irradiation during cloudy conditions. The solar panel's power output was measured also in both the horizontal position and the oriented position given by the eye.

When the solar panel gave a slightly higher voltage of about only +0.8 V than when it is oriented in the horizontal position.

Solar panel's power in horizontal position: **1.119 W**

Solar panel's power when oriented according to the eye: **1.184 W**

The results show an increase of about 6% in the power output. This increase can be significant in large solar power stations and energy production. For example, for a 100 MW power station, assume that the average energy production on a cloudy day is 10000 kWh. An increase of 6% in energy production will give 600 kWh extra, assuming a house consumes 6 kWh/day. This means that the power station can provide energy for 100 more houses on that day.

Chapter 5

Conclusion and Future work

When this topic was first thought of, a realization of nature's creation resembled in insects' eyes was imagined. Creating mechanical, electrical and electronic systems that are capable of simulating living organisms' biological processes and behaviors and making use of it in the renewable energy field was this project's major motivation. Throughout the project, one of nature's most complex biological systems was represented through technical implementations and engineering realizations.

5.1 Results summary

The Arduino mega was found to be successful in representing the insect's brain function of receiving signals from the multiplexer circuit that rotates on the photodiodes and combining them to form an image.

Photodiodes have proven their effectiveness in mimicking different properties of the ommatidia. They were successful in detecting the minimal difference in irradiance coming from the sun giving the advantage of detecting the maximum point of radiation using the insect eye sensor even in cloudy conditions. The solar panel's power output increased by approximately 6% from the horizontal position to the oriented position given by the eye. This increase is significant in large power stations.

5.2 Future work

The results of the prototype are a motivation to continue working on improving the preliminary implementation to give more robust results. There are various approaches of optimizing the artificial compound insect eye sensor mentioned in the following:

5.2.1 Variable resistance in the multiplexer circuit

A problem faced in this project was the fixed resistance in the multiplexer circuit. The results show that the sensitivity of the photodiodes need to be changed according to the weather conditions. A good field of research would be designing a multiplexer circuit in which the resistance can be varied and controlled to suit the environment outside the eye. This can be seen in the human eye for example, where the pupil enlarges and contracts according to the light intensity in the surrounding environment adapting to it. Using a circuit that imitates this phenomena will achieve tracking in clear and cloudy conditions even when very weak light is present, with the help of a large resistance it can be previewed.

5.2.2 Increasing the amount of pixels

In this project a flexible circuit was used to hold the photodiodes. Using the same multiplexer circuit, it is easy to achieve 480 sensors working together or even more. Each Multiplexer circuit uses only 3 analog input pins in the Arduino Mega 2560 which has 16 analog inputs. Using the same ideas, it would be easy to go up to 480 without effort. Increasing the amount of photodiodes gives a higher accuracy in detecting where the maximum irradiance is coming from.

5.2.3 Robust connections

In this project THT pin connectors were used in the flexible circuit. The edges of these connectors affected the circuit and cut some routes. One solution could be the use of a rigid-flex circuit, this will eliminate connections between circuits and there will be no need for cables. Rigid-flex circuits may have fixation problems and might be costly. Another solution would be using SMD connectors instead of THT connectors or a built-in connector in the circuit having a shape of a male header at the edges of the flexible circuit or any another type of connection as the connection used in keyboards in laptops.

5.2.4 Integration and comparison

This project was successful in forming the steps of manufacturing the sensor and proving the concept of detecting the maximum radiation in cloudy conditions, although some problems aroused, but they could be prevented and improved by further research. The next step in this project is to integrate the sensor with the movement of the solar panel to be able to get accurate results that can be compared with sensors already in the market.

Bibliography

[1] M. Srinivasan, J. Chahl, K. Weber, S. Venkatesh, M. Nagle and S. Zhang, 'Robot navigation inspired by principles of insect vision', *Robotics and Autonomous Systems*, vol. 26, no. 2-3, pp. 203-216, 1999.

[2] S. Deepthi, A. Ponni, R. Ranjitha and R. Dhanabal, 'Comparison of Efficiencies of Single-Axis Tracking System and Dual-Axis Tracking System with Fixed Mount', *International Journal of Engineering Science and Innovative Technology (IJESIT)*, vol. 2, no. 2, 2013.

[3] U. Okpeki and S. Otuagoma, 'Design and Construction of a Bi–Directional Solar Tracking System.', *International Journal Of Engineering And Science*, vol. 2, no. 5, pp. 32-38, 2013.

[4] C. Lee, P. Chou, C. Chiang and C. Lin, 'Sun Tracking Systems: A Review', *Sensors*, vol. 9, no. 5, pp. 3875-3890, 2009.

[5] F. Rubio, M. Ortega, F. Gordillo and M. López-Martínez, 'Application of new control strategy for sun tracking', *Energy Conversion and Management*, vol. 48, no. 7, pp. 2174-2184, 2007.

[6] J. Yoo, Y. Kang, B. Song and J. Song, 'Solar Tracking System Experimental Verification Based on GPS and Vision Sensor Fusion', *Journal of Automation and Control Engineering*, vol. 2, no. 4, pp. 417-421, 2014.

[7] J. Duffie and W. Beckman, *Solar engineering of thermal processes*. New York: Wiley, 1980.

[8] J. Clark and H. Ayoub, 'Improving the energy capture of solar collectors', Ph.D, MSc., University of Strathclyde, 2012.

[9] T. Haalboom and A. Boktor, 'Artificial compound insect eye', Ph.D, BSc., Duale Hochschule Karlsruhe.

[10] Watchingtheworldwakeup.blogspot.de, 'Watching the World Wake Up: The Amazing Housefly Part 2: Coolest Eye Ever', 2009. [Online]. Available: http://watchingtheworldwakeup.blogspot.de/2009/11/amazing-housefly-part-2-coolest-eye.html. [Accessed: 08- Apr- 2015].

[11] R. Völkel, M. Eisner and K. Weible, 'Miniaturized imaging systems', *Microelectronic Engineering*, vol. 67-68, pp. 461-472, 2003.

[12] A. Briscoe, 'Reconstructing the ancestral butterfly eye: focus on the opsins', *Journal of Experimental Biology*, vol. 211, no. 11, pp. 1805-1813, 2008.

[13] Park DJ, Karesh JW. 'Topographic anatomy of the eye: an overview. ' In: Tasman W, Jaeger EA (eds). Duane's Ophthalmology on DVD-rom. *Journal of Foundations of Ophthalmology* Volume 1. 2009 edition: Lippincott Williams& Wilkins.

[14] D. Judd and G. Wyszecki, *Color in business, science, and industry*. New York: Wiley, 1975.

[15] L. DeWerd, 'Solid-state electrophotography with Al2O3', *Med. Phys.*, vol. 5, no. 1, p. 23, 1978.

[16] Wikipedia, 'Photo-multiplier', 2015. [Online]. Available: https://en.wikipedia.org/wiki/Photo-multiplier. [Accessed: 15- Mar- 2015].

[17] H. Zeller, 'Cosmic ray induced failures in high power semiconductor devices', *Solid-State Electronics*, vol. 38, no. 12, pp. 2041-2046, 1995.

[18] Radio-electronics.com, 'Phototransistors | Photo Transistor Tutorial | Radio-Electronics.Com', 2015. [Online]. Available: http://www.radio-electronics.com/info/data/semicond/phototransistor/photo_transistor.php. [Accessed: 15- Mar- 2015].

[19] Media.digikey.com, 2015. [Online]. Available: http://media.digikey.com/Photos/Everlight%20Electronics/PD333-3C%5EH0%5EL2.jpg. [Accessed: 26- Aug- 2015].

[20] J. Cox, *Fundamentals of linear electronics*. Albany: Delmar Publishers, 1998.

[21] J. Reed, 'Through-Hole vs. Surface Mount', *Blog.optimumdesign.com*, 2015. [Online]. Available: http://blog.optimumdesign.com/through-hole-vs-surface-mount. [Accessed: 10- Apr- 2015].

[22] Eu.mouser.com, 'Vishay Semiconductors Silicon Phototransistors and Photodiodes | Mouser', 2015. [Online]. Available: http://eu.mouser.com/newproducts/newproductsmanufacturers.aspx?mfg=vishay&virtualdir=vishaysiliconphototd%2f. [Accessed: 26- Aug- 2015].

[23] Radio-electronics.com, 'What is SMT | Surface Mount Technology | Devices SMD | Radio-Electronics.com', 2015. [Online]. Available: http://www.radio-electronics.com/info/data/smt/what-is-surface-mount-technology-tutorial.php. [Accessed: 11- Apr- 2015].

[24] Tech-faq.com, 'What is a Phototransistor?', 2015. [Online]. Available: http://www.tech-faq.com/what-is-a-phototransistor.html. [Accessed: 26- Aug- 2015].

[25] D. Shin and I. Eom, 'A Pair of Light Emitting Diodes for Absorbance Measurement', *Bulletin of the Korean Chemical Society*, vol. 34, no. 10, pp. 3150-3152, 2013.

[26] Reefcentral.com, 'question about combining LED wavelengths - Reef Central Online Community', 2015. [Online]. Available: http://www.reefcentral.com/forums/showthread.php?p=23946896. [Accessed: 26- Aug- 2015].

[27] Sqa.org.uk, '1f: Principles of Data Communications: Multiplexing Techniques - Table of Contents', 2015. [Online]. Available: http://www.sqa.org.uk/e-learning/NetTechDC01FCD/index.htm. [Accessed: 17- Apr- 2015].

[28] Wikipedia, 'Multiplexing', 2015. [Online]. Available: https://en.wikipedia.org/wiki/Multiplexing. [Accessed: 17- Apr- 2015].

[29] 'Flexible Electronics', *Electronic Materials: Science & Technology*, 2009.

[30] Vortex Flex Resources, 'Vortex Flex Resources', 2015. [Online]. Available: https://flexiblecircuittechnologies.wordpress.com/. [Accessed: 15- May- 2015].

[31] L. Keith Arauo - Epec, 'Types of Flex Circuits - Single Sided and Multi-Layer Rigid-Flex PCB's', *Epectec.com*, 2015. [Online]. Available: http://www.epectec.com/flex/types/. [Accessed: 15- May- 2015].

[32] Ultimaker.com, 'Ultimaker 2 | Ultimaker', 2015. [Online]. Available: https://ultimaker.com/en/products/ultimaker-2-family/ultimaker-2. [Accessed: 17- May- 2015].

[33] Rredc.nrel.gov, 'U.S. Solar Radiation Resource Maps', 2015. [Online]. Available: http://rredc.nrel.gov/solar/old_data/nsrdb/1961-1990/redbook/atlas/Table.html. [Accessed: 29- Jul- 2015].

[34] Solarwiki.ucdavis.edu, 'VI. The Sun's Motion - SolarWiki', 2013. [Online]. Available: http://solarwiki.ucdavis.edu/The_Science_of_Solar/Solar_Basics/B._Basics_of_the_Sun/VI._The_Sun's_Motion. [Accessed: 21- Sep- 2015].

[35] A. Luque and S. Hegedus, *Handbook of photovoltaic science and engineering*. Hoboken, NJ: Wiley, 2003.

[36] Commons.wikimedia.org, 'File:From a solar cell to a PV system.svg - Wikimedia Commons', 2014. [Online]. Available: https://commons.wikimedia.org/wiki/File:From_a_solar_cell_to_a_PV_system.svg. [Accessed: 26- Aug- 2015].

[37] D. Sawicz, *HOBBY SERVO*. pp. 1-10.

Annex A

Schematics, tables and pictures

A.1 Mechanical parts schematic

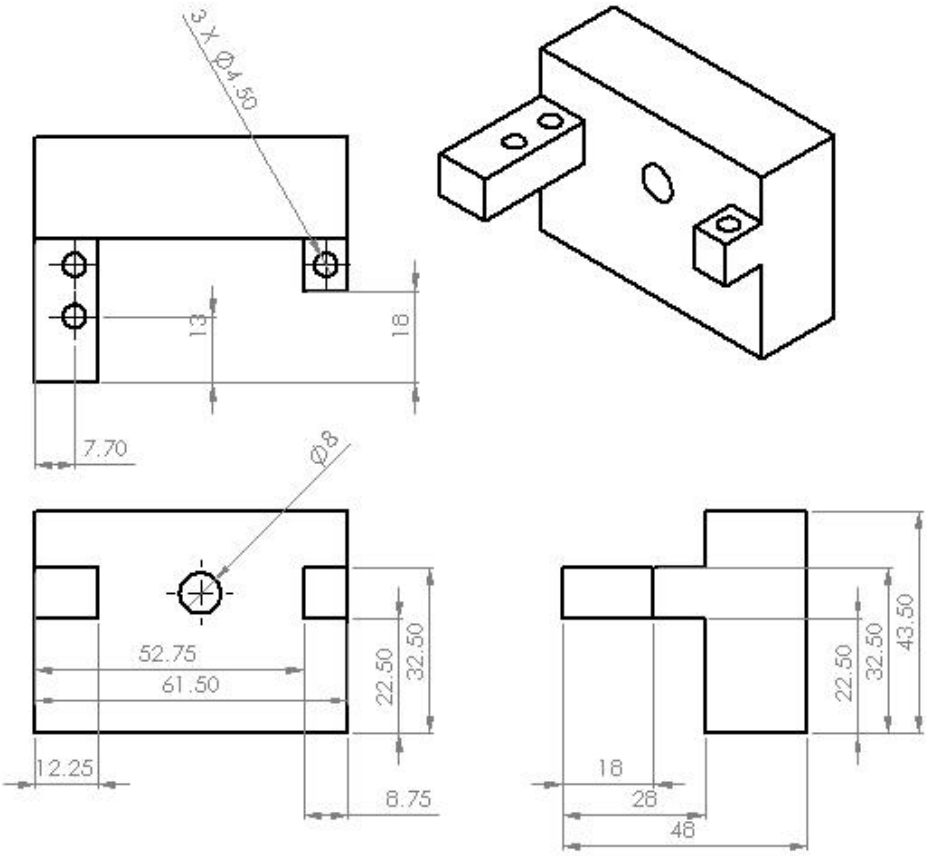

Schematic of the lower part connecting the 2 motors

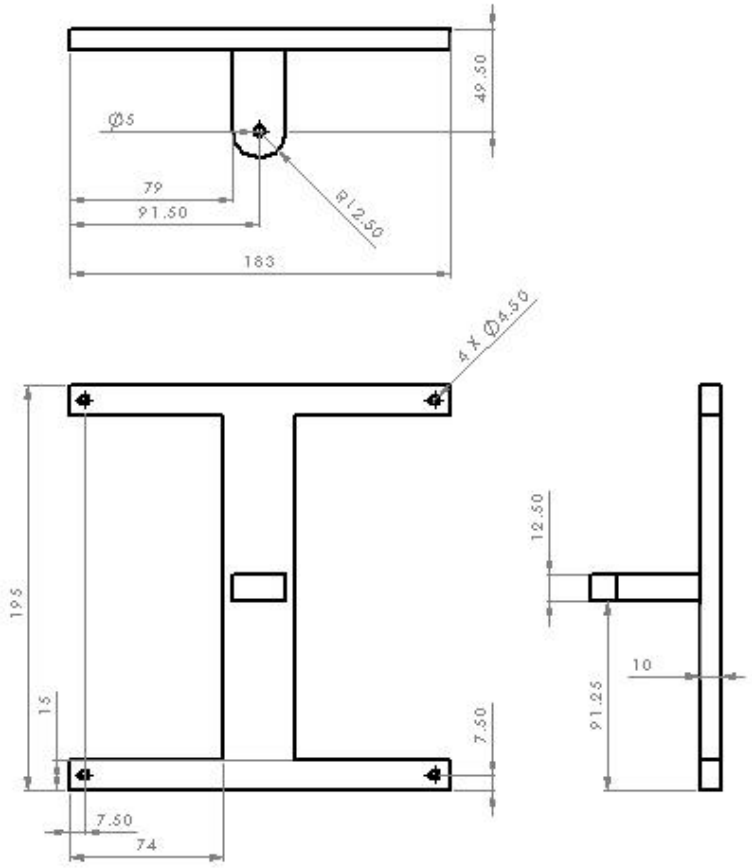

Schematic of the I-shaped part connecting the solar panel to the tilt motor

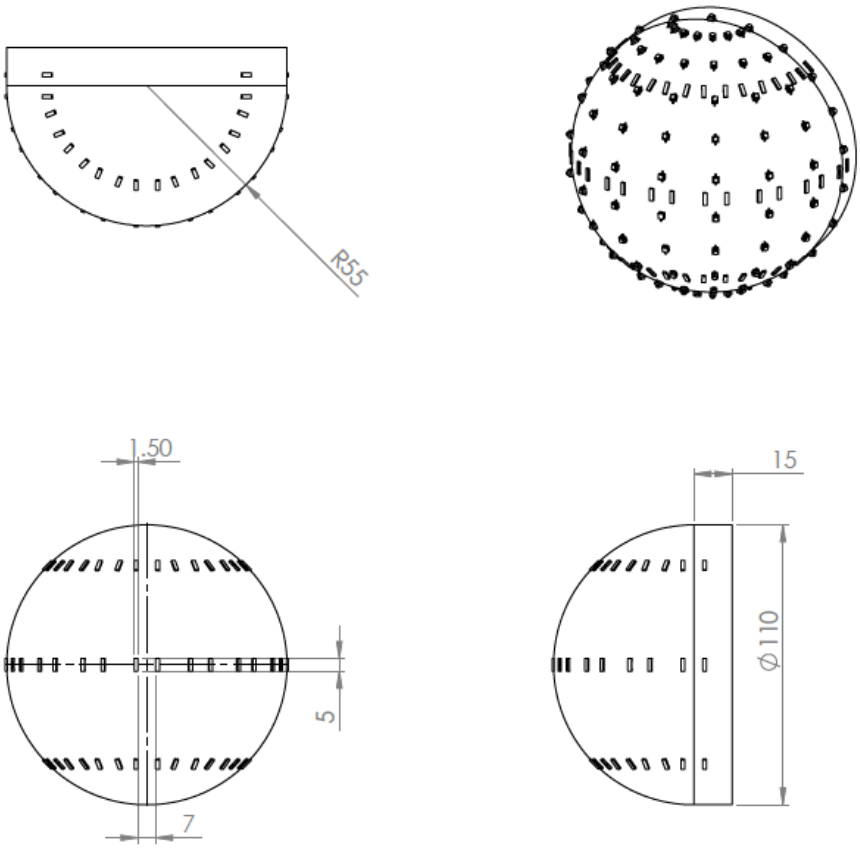

Hemi-spherical eye schematic

A.2 Electrical parts schematics

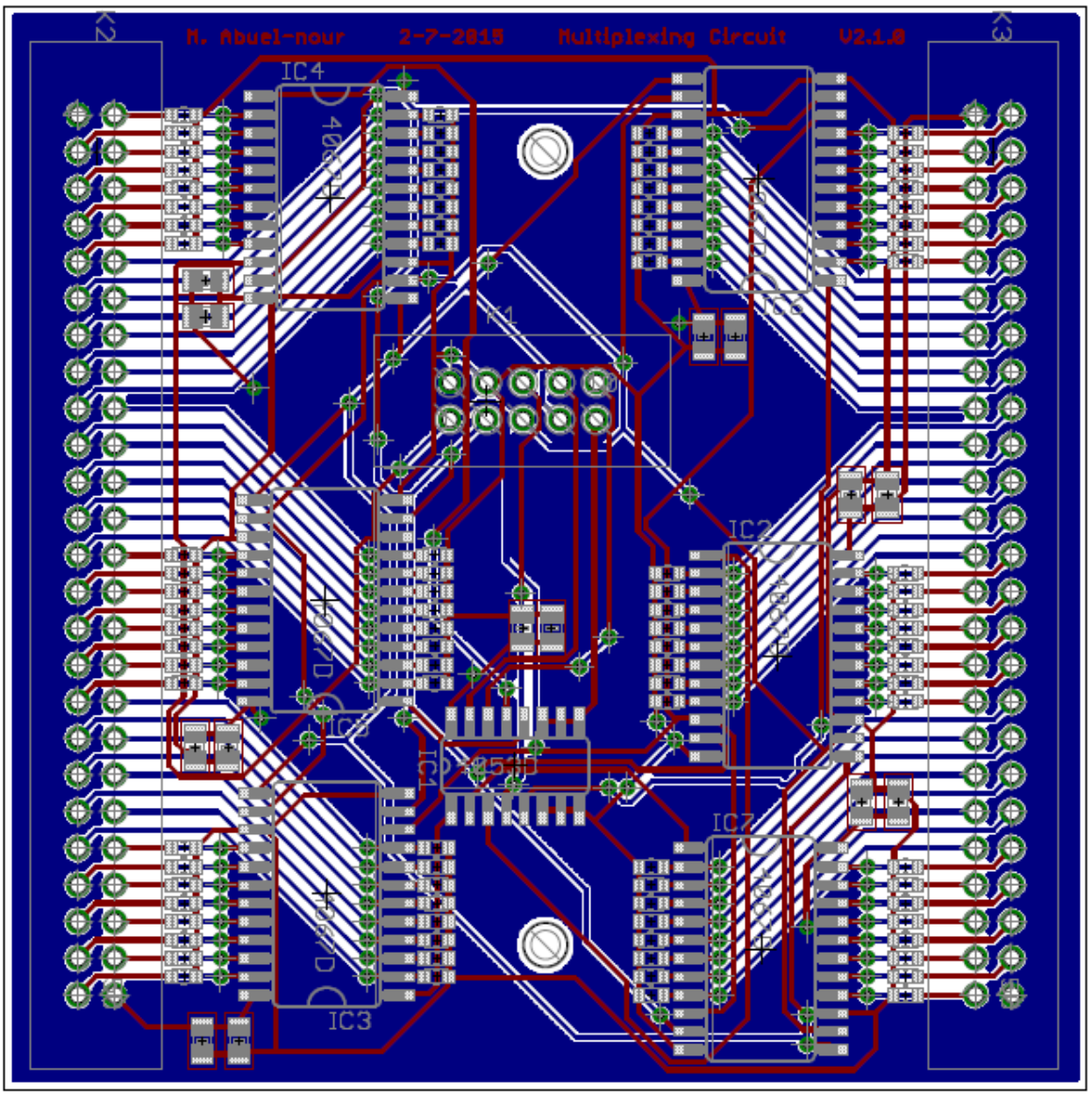

Multiplexing circuit board layout

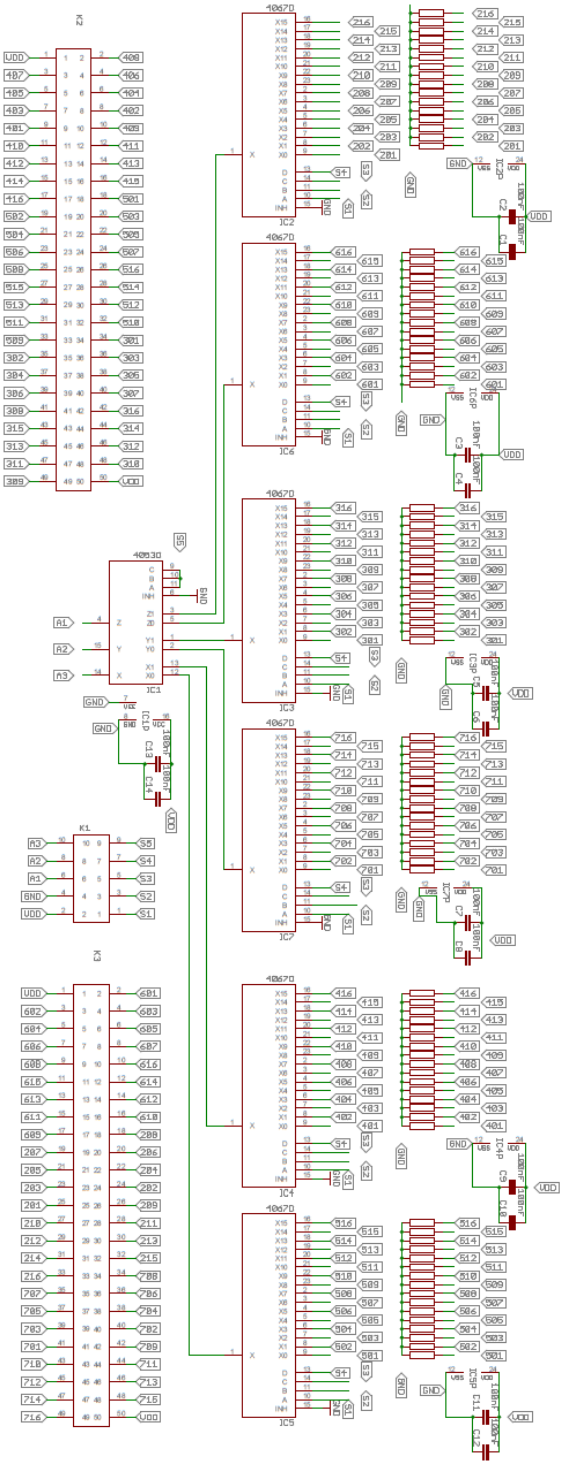

Multiplexing circuit schematic

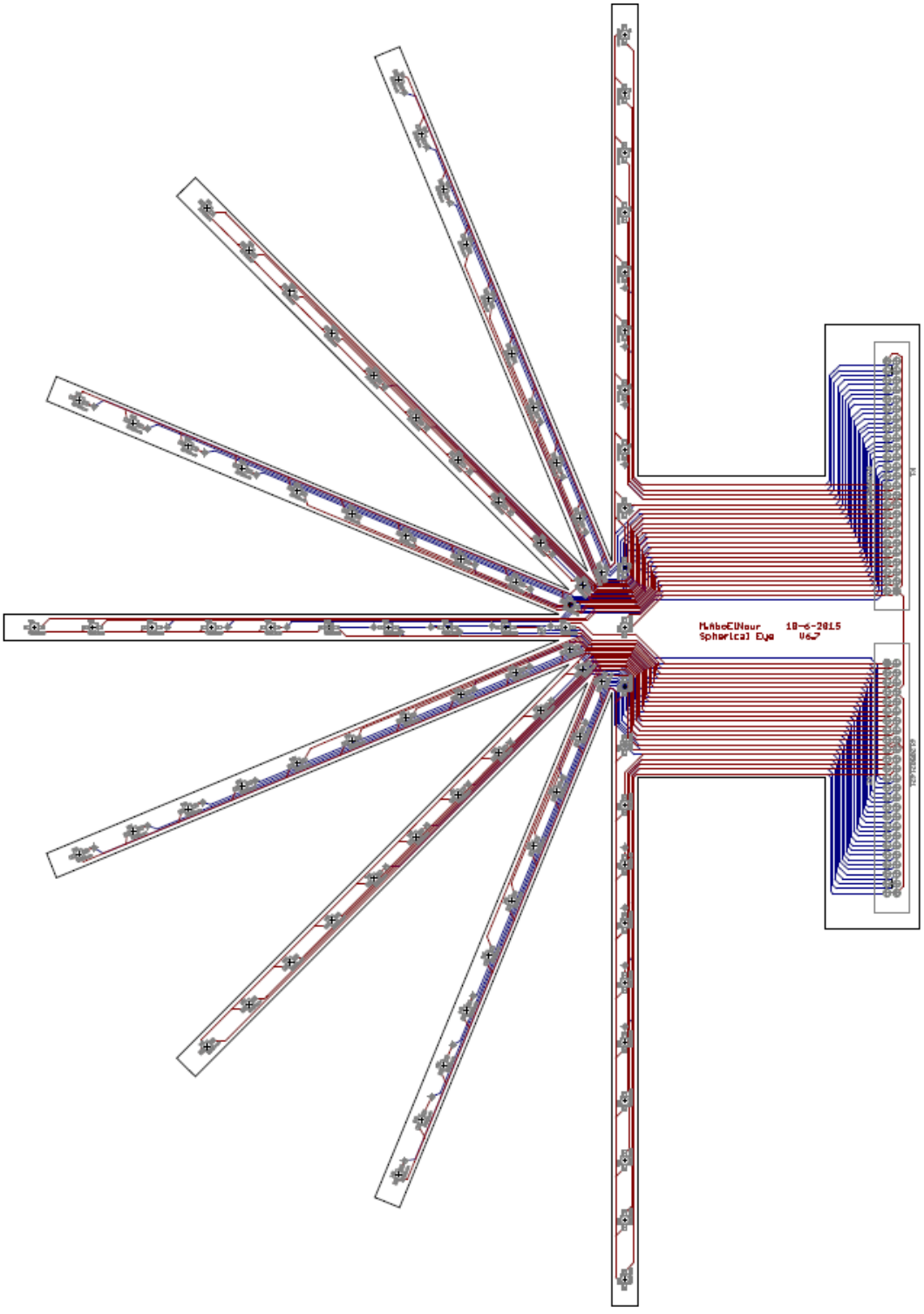

Hemispherical circuit board layout

Hemispherical circuit schematic

A.3 Tables

Multiplexer board pin mapping:

Pin	IC-No.	Pin	IC-No.	Pin	IC-No.	Pin	IC-No.
1	6-01	26	VDD	51	4-08	76	VDD
2	6-03	27	6-02	52	4-06	77	4-07
3	6-05	28	6-04	53	4-04	78	4-05
4	6-07	29	6-06	54	4-02	79	4-03
5	6-16	30	6-08	55	4-09	80	4-01
6	6-15	31	6-14	56	4-11	81	4-10
7	6-13	32	6-12	57	4-13	82	4-12
8	6-11	33	6-10	58	4-15	83	4-14
9	2-08	34	6-09	59	5-01	84	4-16
10	2-06	35	2-07	60	5-02	85	5-03
11	2-04	36	2-05	61	5-04	85	5-05
12	2-02	37	2-03	62	5-06	87	5-07
13	2-09	38	2-01	63	5-16	88	5-08
14	2-11	39	2-10	64	5-14	89	5-15
15	2-13	40	2-12	65	5-12	90	5-13
16	2-15	41	2-14	66	5-10	91	5-11
17	7-08	42	2-16	67	3-01	92	5-09
18	7-06	43	7-07	68	3-02	93	3-03
19	7-04	44	7-05	69	3-04	94	3-05
20	7-02	45	7-03	70	3-06	95	3-07
21	7-09	46	7-01	71	3-16	96	3-08
22	7-11	47	7-10	72	3-14	97	3-15
23	7-13	48	7-12	73	3-12	98	3-13
24	7-15	49	7-14	74	3-10	99	3-11
25	VDD	50	7-16	75	VDD	100	3-09

Hemi-spherical eye diode location mapping:

Diode	Pin	Diode	Pin	Diode	Pin	Diode	Pin
1	27	26	14	46	48	71	7
2	28	27	15	47	24	72	8
3	29	28	16	48	25	73	9
4	30	29	17	49	26	74	10
5	2	30	40	50	49	75	37
6	3	31	18	51	18	76	36
7	4	32	19	52	19	77	35
8	5	33	20	53	20	78	12
9	6	34	21	54	21	79	11
10	32	35	46	55	47	80	34
11	7	36	45	56	46	81	28
12	8	37	43	57	45	82	29
13	9	38	23	58	23	83	30
14	36	39	22	59	22	84	2
15	35	40	44	60	44	85	3
16	34	41	47	61	38	86	4
17	12	42	48	62	39	87	5
18	11	43	24	63	40	88	31
19	10	44	25	64	42	89	6
20	33	45	26	65	13	90	33
21	37	91	49	66	14	92	27
22	38	VDD	1	67	15	VDD	1
23	39	VDD	31	68	16	VDD	32
24	41	VDD	42	69	17	VDD	43
25	13	VDD	50	70	41	VDD	50

A.4 Pictures

The following pictures shows the steps required to produce a PCB in general:

1. Solder paste was put on the circuit pads either manually or using stencil.

Stencil

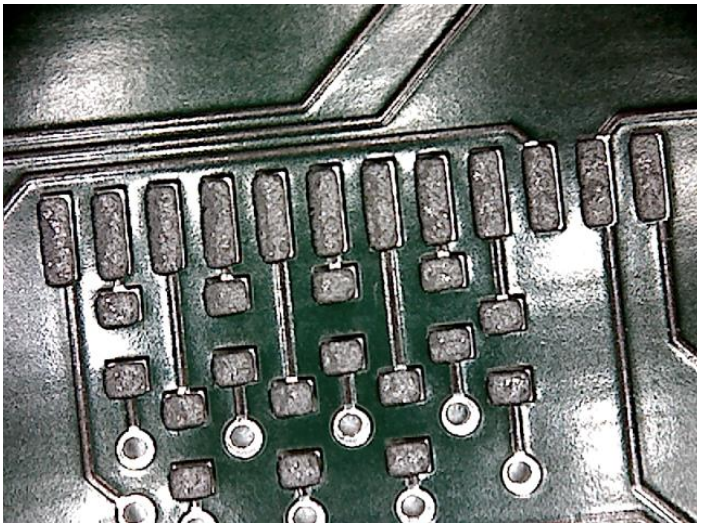

Solder paste on the PCB

2. The pick and place machine - FRITSCH SM 902 - was used to put the SMD components on the solder paste.

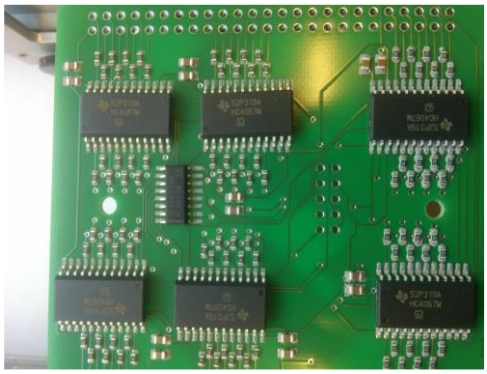

SMD components on the PCB

3. The PCB was put in the vapor phase technology machine ASSCON QUICKY 300 to solidify the solder paste for 12 min.

ASSCON QUICKY 300

4. The circuit is removed and the THT components were soldered and the circuit was taken for experimentation.

Annex B

Codes

B.1 Arduino code

```
byte controlPins[] ={ B00000000, B00000001, B00000010, ... , B00011111};
                                    //From binary 0 to 31

int pixelMap [10][9]; //2D array for the sensors
int pixel91;
int pixel92;


void setup()
{
  Serial.begin(9600);
  DDRA = B11111111; // set PORTA (digital 7~0) to outputs
}

void setPin(int outputPin) //choosing the combination of selection lines
{
  PORTA = controlPins[outputPin];
}

int getA0 () //reading analog signal from analog input A0
{
  return analogRead(A0)/4;
}

int getA1 () //reading analog signal from analog input A1
{
  return analogRead(A1)/4;
}

int getA2 () //reading analog signal from analog input A2
{
  return analogRead(A2)/4;
}


void mapping() //reading each time the value of 3 sensors, then changing the
               //selection lines, each time mapping the sensor to the correct
               //position in the 2D array
{
setPin(0);
pixelMap [9][4] = getA0(); pixelMap [3][7] = getA1(); pixelMap [0][3] = getA2();

setPin(1);
pixelMap [5][4] = getA0(); pixelMap [8][7] = getA1(); pixelMap [1][3] = getA2();

setPin(2);
pixelMap [4][5] = getA0(); pixelMap [7][7] = getA1(); pixelMap [2][3] = getA2();

setPin(3);
pixelMap [5][5] = getA0(); pixelMap [4][6] = getA1(); pixelMap [3][3] = getA2();

...
```

```
setPin(31);
pixelMap [0][5] = getA0(); pixelMap [8][1] = getA2();

}

void loop()
{
    mapping(); //filling the array with the sensor readings
    int b = 0;
    int bx = 0;
    int by = 0;
  for(int j = 0; j < 10; j++) { //sending data with serial communication
    for (int i = 0; i < 9; i++) {
      if(pixelMap[i][j] > b){
        b = pixelMap[i][j];
        bx = i;
        by = j;
      }
    }
  }

   for(int j = 0; j < 9; j++) {
    for (int i = 0; i < 10; i++) {
      Serial.print(pixelMap[i][j]);
      if (i * j < 72) {
        Serial.print(", ");
      }
    }
  }
  Serial.println();

  if (pixel91 > b){
    b = pixel91;
    bx = 9;
    by = 1;
  }
  if (pixel92 > b){
    b = pixel92;
    bx = 9;
    by = 2;
  }
delay(100);
}
```

B.2 MATLAB code

```
    clear all;
    clc
    s1 = serial('COM7');                              %define serial port
    s1.BaudRate=9600;                                 %define baud rate
    fclose(s1);

    global KEY_PRESS
    KEY_PRESS = 0;
    f = figure();
    set(f, 'KeyPressFcn', @myKeyPressFcn);

    fopen(s1); %open serial port
    s1.ReadAsyncMode = 'continuous';
```

```
readasync(s1);
while(s1.BytesAvailable <= 0)  %wait until Arduino outputs data
end
while KEY_PRESS %read untill key is pressed
        data = fscanf(s1); %read sensor
        flushinput(s1);
        splitData = strsplit(data,', '); %split CSV to single data
        doubleVector = str2double(splitData); %convert to double
        matrix = vec2mat(doubleVector, 10); %obtain the matrix
        imag = mat2gray(matrix, [0 255]); %convert to gray scale image
        imshow(imag,'InitialMagnification','fit') %enlarge the preview
        drawnow %update image preview
end
% close the serial port!
fclose(s1);
```